

ornl

MARTIN MARIETTA ENERGY SYSTEMS LIBRARIES



3 4456 0315272 7

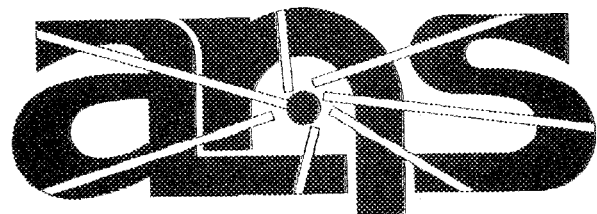
ORNL/TM-11324

**OAK RIDGE
NATIONAL
LABORATORY**

MARTIN MARIETTA

**Steam-Explosion Safety Considerations
for the Advanced Neutron Source
Reactor at the Oak Ridge
National Laboratory**

Rusi Taleyarkhan



Advanced Neutron Source

OAK RIDGE NATIONAL LABORATORY

CENTRAL RESEARCH LIBRARY

CIRCULATION SECTION

459M ROOM 171

LIBRARY LOAN COPY

DO NOT TRANSFER TO ANOTHER PERSON

If you wish someone else to see this report, send us name with report and the library will arrange a loan.

OPERATED BY
MARTIN MARIETTA ENERGY SYSTEMS, INC.
FOR THE UNITED STATES
DEPARTMENT OF ENERGY

This report has been reproduced directly from the best available copy.

Available to DOE and DOE contractors from the Office of Scientific and Technical Information, P.O. Box 62, Oak Ridge, TN 37831; prices available from (615) 576-8401, FTS 626-8401.

Available to the public from the National Technical Information Service, U.S. Department of Commerce, 5205 Port Royal Rd., Springfield, VA 22161.

NTIS price codes--Printed Copy: A05 Microfiche A01

This report was prepared as an account of work sponsored by an agency of the United States Government. Neither the United States Government nor any agency thereof, nor any of their employees, makes any warranty, express or implied, or assumes any legal liability or responsibility for the accuracy, completeness, or usefulness of any information, apparatus, product, or process disclosed, or represents that its use would not infringe privately owned rights. Reference herein to any specific commercial product, process, or service by trade name, trademark, manufacturer, or otherwise, does not necessarily constitute or imply its endorsement, recommendation, or favoring by the United States Government or any agency thereof. The views and opinions of authors expressed herein do not necessarily state or reflect those of the United States Government or any agency thereof.

ORNL/TM-11324

Oak Ridge Severe Accident Analysis Program
Engineering Technology Division

STEAM-EXPLOSION SAFETY CONSIDERATIONS FOR THE
ADVANCED NEUTRON SOURCE REACTOR AT
THE OAK RIDGE NATIONAL LABORATORY

Rusi Taleyarkhan

Manuscript Completed - October 1989
Date Published - February 1990

Prepared by the
OAK RIDGE NATIONAL LABORATORY
Oak Ridge, Tennessee 37831
operated by
MARTIN MARIETTA ENERGY SYSTEMS, INC.
for the
U.S. DEPARTMENT OF ENERGY
under contract DE-AC05-84OR21400



3 4456 0315272 7

CONTENTS

	<u>Page</u>
FOREWORD	v
ACKNOWLEDGMENTS	vii
LIST OF TABLES	ix
LIST OF FIGURES	xi
GLOSSARY	xiii
ABSTRACT	1
1. INTRODUCTION	2
1.1 IMPORTANCE OF STUDY	2
1.2 HISTORICAL BACKGROUND	2
1.3 STEAM-EXPLOSION PHENOMENA	3
2. STEAM-EXPLOSION EXPERIMENTS	6
2.1 REACTOR EXPERIMENTS	6
2.2 OUT-OF-REACTOR EXPERIMENTS	7
3. CONVENTIONAL STEAM-EXPLOSION ANALYSIS FOR LWRs	13
3.1 FUEL-COOLANT MIXING	13
3.2 TRIGGERING	13
3.3 PROPAGATION	16
3.4 EXPANSION	18
3.5 FAILURE ANALYSIS	19
3.5.1 Response to Initial Pressure Pulse	19
3.5.2 Response to Slug Loading	20
3.5.3 Missile Generation	22
3.5.4 Ex-vessel Steam Explosions	22
3.6 PROBABILITY OF CONTAINMENT FAILURE	22
4. MODELING AND BENCHMARKING FOR ANS STUDY	25
5. PRELIMINARY STEAM-EXPLOSION ANALYSIS FOR ANS	30
5.1 ESTIMATED ANS STEAM-EXPLOSION LOADINGS	30
5.2 ANS FAILURE ANALYSIS AND DESIGN IMPLICATIONS	34
6. SUMMARY AND CONCLUSIONS	40
6.1 PROPENSITY FOR ENERGETIC STEAM-EXPLOSION OCCURRENCE IN ANS	40
6.2 DAMAGE POTENTIAL FROM STEAM EXPLOSIONS IN ANS	41

	<u>Page</u>
6.3 EXTENT OF ANALYSIS FOR ANS	42
6.4 MODELING OF DESTRUCTIVE LOADINGS FROM STEAM EXPLOSIONS VS CHEMICAL DETONATIONS	42
7. RECOMMENDATIONS	43
REFERENCES	45
APPENDIX A. NOTES ON ANS CORE-DISRUPTION THERMODYNAMICS	49
A.1 ALUMINUM AND U ₃ Si ₂ PROPERTIES	49
A.2 ENERGY REQUIREMENTS	49
A.3 CORE DISRUPTION TIMES	51
A.4 LIMITS ON POWER EXCURSIONS AND HEATUPS	52
A.4.1 Reactivity Excursion Without Scram	52
A.4.2 Inadequate Cooling Without Scram	53
A.4.3 Inadequate Cooling after Scram (Decay Heat Power)	53
A.5 STEAM EXPLOSION VS RAPID STEAM GENERATION	54
A.6 ENERGY AVAILABLE FOR STEAM EXPLOSION IN CPBT	55
APPENDIX B: HYPOTHETICAL REACTIVITY EXCURSION WITHOUT SCRAM: LIMITING DEBRIS TEMPERATURE AND ENERGY ESTIMATES	59
B.1 INTRODUCTION	59
B.1.1 Containment Design Criteria	59
B.1.2 Implied Design Criteria	59
B.1.3 Reactivity Accident-Selection Criteria	59
B.1.4 Input Data Needed for Fuel-Coolant Interaction Calculations	59
B.2 CALCULATIONAL ASSUMPTIONS	60
B.3 CALCULATIONS FOR THE \$1.00/s RAMP REAC- TIVITY INSERTION WITHOUT SCRAM	60
B.4 UNCERTAINTY ANALYSIS	62
APPENDIX C. WORKSHOP ON CAUSES AND PREVENTION OF MELT-WATER EXPLOSIONS	63
C.1 WORKSHOP PARTICIPANTS	63
C.2 OVERALL CONCLUSIONS/MESSAGE OF WORKSHOP	63

FOREWORD

The goal of the Advanced Neutron Source (ANS) severe accident analysis effort is to provide a constructive and positive mechanism for development of an ANS design that is resistant to severe accidents, capable of recovering from potential severe accident initiators before the onset of a core-melt accident, and capable of protecting the public health and safety in the unlikely event that a severe accident were to occur. This goal will be achieved through implementation of lessons learned from commercial reactor safety research and experimental and test reactor experience and application of state-of-the-art analysis tools and methods for the development of the best possible understanding of ANS severe accident performance. This report represents the first of a series of ANS severe accident issue papers designed to (1) identify potential ANS severe accident phenomenological issues at a very early stage in the ANS design effort, (2) provide simplified scoping analyses and to define the issues and associated uncertainties, (3) identify ANS design decisions that have the potential to affect the probability and/or magnitude of severe accident phenomena, and (4) suggest a framework for future resolution of the various issues identified. It is not the intent, therefore, of these reports to provide definitive analyses, but rather to provide a mechanism by which severe accident issues may be effectively addressed during the design process.

Future ANS severe accident issue papers will deal with (1) post-melt fuel behavior (material relocation and coolability), (2) the ANS fuel fission-product release and transport phenomena under severe accident conditions, (3) U_3Si_2/Al fuel-concrete interactions, (4) applicable lessons learned from light-water reactor and liquid-metal reactor severe accident research, and (5) identification of the various thermodynamic energy sources present within the ANS containment. These issue papers will be used as input to the ANS severe accident modeling assessment and bounding containment loads analysis to be performed during the conceptual design phase of the ANS Project.

Sherrell R. Greene
Program Manager
Oak Ridge Severe Accident
Analysis Program

ACKNOWLEDGMENTS

The author wishes to acknowledge the contributions made by various individuals to this report. R. C. Gwaltney and C. R. Luttrell evaluated the structural response characteristics of the core pressure boundary tube and the reflector tank. R. M. Harrington contributed Appendices A and B, which deal with the evaluation of thermal energy levels and temperatures of molten fuel under postulated accident scenarios. The in-depth review and critique provided by S. R. Greene, R. M. Harrington, C. D. West, and H. Reutler has greatly assisted in improving the quality of this document. The author also wishes to thank M. Lee Hyder (Savannah River Laboratory) and Lloyd Nelson (Sandia National Laboratory) for helpful discussions on the characteristics of aluminum-water interactions. Finally, the sponsorship and active support for this work provided by C. D. West and R. M. Harrington of the Advanced Neutron Source Project Office is gratefully acknowledged.

LIST OF TABLES

<u>Table</u>		<u>Page</u>
1	Characteristic features of steam and chemical explosions	4
2	Open geometry experimental observations	9
3	FITS experimental observations	10
4	Summary of commercial LWR vessel-failure evaluation	22
5	Model verification calculations	26
6	Model benchmarking calculations with experiments	27
7	Initial conditions for preliminary ANS calculations	30
8	Comparison of pressure-pulse magnitudes from steam explosions with chemical detonations	32
9	Limiting pressure-pulse magnitudes for CPBT and reflector tank fabricated with various materials	37
10	Estimates of ANS RCS pressurization levels from expansion phase of steam explosions	38
11	Estimates of ANS slug energetics from expansion phase of steam explosions	39
A.1	Hypothetical ANS core-disruption times	51

LIST OF FIGURES

<u>Figure</u>		<u>Page</u>
1	Postulated steam-explosion scenario for commercial LWRs	7
2	Schematic representation of interaction vessel used in open-geometry steam-explosion experiments	8
3	Schematic representation of FITS experimental setup	14
4	Explosion-conversion ratio and debris diameter as function of coolant-to-mass ratio	15
5	Explosion-conversion ratio and debris diameter as function of mixture-to-fuel volume ratio	15
6	Comparison of calculation and data for FITS test MD-19	17
7	Failure envelope for lower plenum under initial pressure-pulse loading immediately after steam explosion, cases 1 and 2	17
8	Schematic representation for 1-D expansion model	18
9	Structural model and locations of failure for LWR steam-explosion-related failure evaluation	20
10	Steam-explosion loading mechanisms for expansion phase of steam-explosion transient	21
11	Frequency of containment failure vs missile energy for LWR analysis	24
12	Schematic representation of molten aluminum-water steam-explosion experiment T122 at Winfrith	27
13	Variation of peak pressure-pulse magnitudes vs fuel temperatures, coolant-to-fuel mass ratio = 1.0	31
14	Variation of peak pressure-pulse magnitudes vs fuel temperatures, coolant-to-fuel mass ratio = 0.5	31
15	ANS slug energetics during expansion phase	33
16	RCS loop-pressurization parametrics	33
17	ANS failure envelopes for CPBT and reflector tank	35

GLOSSARY

ANS	Advanced Neutron Source
ATWS	Anticipated transient without scram
Corium-A	A simulant of a whole LWR core and all the lower in-vessel support structure if it were molten
Corium-A+R	Same as Corium-A, with steel added to simulate a mixture that includes material from the reactor vessel bottom head
Corium-E	A simulation of molten core and all structural material within the reactor vessel of a LWR
Conversion ratio	Ratio of mechanical work measured to the fuel thermal energy
CPBT	Core pressure boundary tube, representing the immediate pressure boundary surrounding the ANS reactor core region
DNB	departure from nucleate boiling
EPRI	Electric Power Research Institute
FCI	fuel-coolant interaction
FITS	fully instrumented test series
IFCI	Integrated Fuel Coolant Interaction Code
LASL	Los Alamos Scientific Laboratory
LWR	light-water reactor
ORNL	Oak Ridge National Laboratory
PETN	Pentonite
PRA	probabilistic risk assessment
PWR	pressurized-water reactor
RCS	reactor coolant system
RPV	reactor pressure vessel
RSS	Reactor Safety Study

SNL	Sandia National Laboratories
SRL	Savannah River Laboratory
STP	standard temperature and pressure
UCSP	upper core support plate

STEAM-EXPLOSION SAFETY CONSIDERATIONS FOR THE ADVANCED
NEUTRON SOURCE REACTOR AT THE OAK RIDGE
NATIONAL LABORATORY

Rusi Taleyarkhan

ABSTRACT

This report provides a perspective on steam-explosion safety and design issues for the Advanced Neutron Source (ANS) reactor being designed at the Oak Ridge National Laboratory.

A historical background along with a description of experiments and analytical work performed to date has been provided. Preliminary analyses (for the ANS) have been conducted to evaluate steam-explosion pressure-pulse loadings, the effects of reactor coolant system (RCS) overpressurization, and slug energetics.

The method used for pressure-pulse magnitude evaluation was benchmarked with previous calculations, an aluminum-water steam-explosion experiment, and test reactor steam explosion data with good agreement. Predicted pressure-pulse magnitudes evaluated were found to be several orders of magnitude lower than corresponding values evaluated by correlating available energies with shock-wave pressures from equivalent chemical detonations.

Parametric calculations were conducted to note pressure-pulse magnitudes, slug energetics, and RCS loop pressurization over a wide range of expected fuel temperatures, coolant-to-fuel mass ratios, void fractions, and mechanical energy levels transferred to coolant and compressible volumes. A failure envelope was generated to evaluate structural integrity at different pressure-pulse magnitude levels, of various pulse durations, for the core pressure boundary tube (CPBT) and reflector tank. Preliminary estimates were generated to note expected pressure-pulse levels for accident scenarios of varying severity. The accident scenarios evaluated were (1) a reactivity excursion without scram, (2) an inadequate primary coolant flow without scram, and (3) an inadequate cooling on decay heat. For all three types of accidents under the assumed conditions, the as-designed CPBT would be incapable of withstanding the pressure pulses generated immediately following a steam explosion. However, the reflector tank may be expected to withstand the pressure pulses from Case 3 with a reasonable safety margin. The integrity of the reflector tank would be severely challenged for Cases 1 and 2, and failure may occur when the coolant void fraction in the explosion zone is not

high (i.e., ~90%). A similar limited-scope failure analysis (using a similarity hypothesis) for two other materials (stainless steel and Zircaloy-2) demonstrated the superior rupture characteristics of these materials.

The preliminary best estimate, as well as conservative estimates for RCS volume-pressurization failure and slug energetics, indicated that (1) steam explosions in the ANS have significant damage potential, and (2) steam-explosion issues must be considered during the design phase of the ANS Project. Recommendations are made for efficiently addressing this important safety and design issue.

1. INTRODUCTION

1.1 IMPORTANCE OF STUDY

It is important to recall that the very idea for an energetic steam explosion stems principally from experiences with destructive steam explosions in plate-type, aluminum-clad research reactors undergoing prompt critical nuclear excursions. This evidence includes the SL-1 incident and both the BORAX-1 and SPERT-1 destructive tests. The characteristics of the proposed Advanced Neutron Source (ANS) reactor core closely parallel those of the previously mentioned reactor cores (see Sect. 2.1); therefore, we plan to give early consideration in the safety analysis of ANS to the potential for destructive steam explosions in the safety analysis of ANS.

Hence, this study is motivated by the need to develop a robust ANS reactor design with an acceptable level of risk to public health and plant investment resulting from steam explosions.

1.2 HISTORICAL BACKGROUND

A problem of historical concern in commercial reactor safety is the possibility of core meltdown-induced energetic fuel-coolant interactions (FCIs). For hypothetical light-water reactor (LWR) core-meltdown accidents, molten core material and water can coexist in a separate state within the reactor pressure vessel (RPV) with the potential for a destructive steam explosion to occur if the two are intimately mixed under specific operating conditions. This issue gained initial prominence through the so-called Reactor Safety Study (RSS) or WASH-1400.¹

In 1975, RSS concluded that, based on probabilistic risk analyses, LWR core-meltdown accidents were the dominant risk contributors to public health and safety. One prime reason for this conclusion was that containment failure and subsequent radioactivity release could be caused

containment failure and subsequent radioactivity release could be caused by steam explosions, also commonly referred to as FCIs. The analytical model used to calculate rupture of RPV in WASH-1400 was based principally on extrapolated experience from small test reactors undergoing prompt critical nuclear excursions (i.e., the BORAX² and SPERT³ destructive tests and the SL-1 incident⁴).⁵ Furthermore, industrial experience with steam explosions caused by accidental spills of molten material into water in metal boundaries⁶ and in the pulp and paper industry⁷ were cited as general support that large-scale steam explosions could occur.

The RSS considered both in-vessel and ex-vessel steam explosions. Energetic in-vessel steam explosions were assumed to cause containment rupture in all accident sequences that led to the most severe radiological release consequences. It was assumed in RSS that the molten fuel was not only predispersed into the water in the RPV lower head but that a coherent liquid slug existed to transmit the energy from the expanding steam to the RPV upper structure, producing high-velocity missiles in the process. Ex-vessel steam explosions were also considered but were deemed insignificant from a safety standpoint.

The previously mentioned study gave rise to an extensive experimental and analytical research program that has evolved over the past decade. This program has led to a greater understanding of the conditions required for large-scale steam explosions to occur. Brief descriptions of these insights will be given in subsequent sections. However, a basic description of steam-explosion phenomena and the applicability of these phenomena to the ANS design is described next to develop the necessary background for subsequent chapters.

1.3 STEAM-EXPLOSION PHENOMENA

A classical steam explosion is defined as a physical, nonchemical phenomenon that results from an extremely rapid thermal energy transfer between two intimately contacted liquids at different temperatures. The temperature of the hottest liquid, usually a molten metal or refractory material, must be far above the normal boiling point of the second liquid to produce explosive vaporization rates that generate the high pressures and shock waves characteristic of an explosion.

Note carefully that steam explosions are fundamentally different from chemical ones.^{6,7} Unlike steam explosions, chemical explosions are driven by rapid chemical reaction rates. Steam explosions require mixing on an explosive time scale, whereas chemical explosives are finely intermixed before the explosion for oxidizing systems or require no intermixing if the chemical reaction is one of decomposition. Table 1 summarizes the differences between steam explosions and chemical detonations. As noted in Table 1, peak pressures from chemical detonations can attain values in the 10^4 -MPa range (i.e., several million pounds per square inch). In contrast, steam-explosion pressure levels are much smaller. Nevertheless, they can damage the pressure boundary if not

Table 1. Characteristic features of steam and chemical explosions

Feature	Steam explosion	Chemical detonations
Mixing	Requires premixing	Finely intermixed before the explosion
Driving force	Rapid thermal energy transfer between hot and cold liquids	Rapid chemical reaction rates
Pressure rise times	Millisecond range	Microsecond range
Peak pressures	100-MPa range	10 ⁵ -MPa range
Main destructive component	Expanding steam	Shock wave

accounted for in the design phase. The severe damage caused by explosives is derived mainly from the shock wave itself. Large steam explosions, in contrast, liberate most of the damage-producing energy through the relatively slowly expanding steam rather than through the shock wave.

Those differences between steam and chemical explosions have been highlighted principally to avoid gross misconceptions that can arise from attempts to evaluate steam-explosion pressure pulses by means of correlation of melt energy levels with detonation experiments.

Large-scale steam explosions occur in four stages:

1. Fuel coolant mixing. The molten fuel and liquid coolant become intermixed on an explosive time scale, whereas the heat-transfer mode is relatively quiescent. This process provides enough surface area of contact between the molten fuel and water to sustain the required high heat-transfer rate.
2. Triggering. The fuel and coolant are brought into near liquid-liquid contact. Thereafter, rapid heat transfer begins. Triggers can be spontaneous or from external stimuli, such as exploding wires or minidetectors.
3. Explosion propagation. The heat-transfer process rapidly escalates as more of the molten metal is fragmented and as more high-pressure coolant vapor is generated. This phenomenon ensures that a sizable fraction of the available explosive work is used. Note that at this stage, significant, potentially destructive, pressure pulses are generated with durations in the millisecond (typically ≤ 5 -ms) range.

4. Expansion. The high-pressure vapor expands against the surroundings with the potential for destructive mechanical work, such as rupturing the RPV. In this stage, a coherent liquid slug with good fluid/structure coupling may be generated if the steam is contained and directed. The liquid slug may become quite energetic if there is a void space that provides a path for acceleration. Containment rupture may occur from contact with this energetic slug of water or with other missiles generated by the slug.

An Electric Power Research Institute-sponsored study^{6,7} has concluded that although the characteristics of the plate-type reactor designs (i.e., SPERT-1, BORAX-1, and SL-1 destructive tests/accidents) were well-suited for destructive steam-explosion occurrences, they were nevertheless fundamentally different from current commercial water-reactor designs, as is the configuration developed during hypothetical core meltdown accidents for the two design concepts. However, the same cannot be said for the ANS when comparing it with the earlier test reactors. The ANS reactor uses closely spaced plate-type aluminum-clad fuel and operates with very high power densities, thus satisfying the necessary criteria for a propagating steam explosion. Thus, the likelihood of failures related to steam explosions in ANS will be considered in the safety analysis. Based on preliminary heatup calculations⁸ performed by R. M. Harrington,* fuel heatup rates can be high enough to cause the occurrence of high-temperature molten aluminum throughout most of the core. Conditions thus seem ideal for the initiation and propagation of energetic, and possibly destructive, steam explosions given the occurrence of a core-melt accident. This aspect (dealt with in some depth later in Chap. 3) clearly underscores the need for a preliminary study and careful investigation of steam explosions from safety and design standpoints.

*Reference 8 has been included as Appendix A.

2. STEAM-EXPLOSION EXPERIMENTS

The purpose of this section is to outline briefly experiments conducted to demonstrate and study steam explosions. Major phenomena and conclusions are also described for completeness. For further information, the reader may consult key references documented in this report.

2.1 REACTOR EXPERIMENTS

The SPERT and BORAX destructive tests and the SL-1 (Refs. 2-5) incident/accident are demonstrative of destructive steam-explosion reactor experiments. The fuel of those reactors was fully enriched ^{235}U alloyed with aluminum (rapid thermal response) and formed into ≈ 0.5 -mm-thick flat plates. These plates were covered with aluminum cladding, allowing fast thermal response (i.e., a thermal time constant equal to or less than the nuclear period). Thus, the fuel and the coolant provided an intimately mixed configuration even before the rapid energy deposition. Therefore, the combination of the initial geometry (i.e., a well-mixed state) and the rapid energy deposition in the fuel provided conditions (molten fuel and cladding sufficiently premixed) ideal for producing a propagating steam explosion. Indeed, the combination of the rapid power excursion and the fuel-design characteristics (initial premixing) eliminated the need for any significant fragmentation and mixing either before or during the explosion. In addition, the coherent liquid-slug requirement was satisfied because the systems were almost full of cold water before the nuclear excursion. This situation provided a means for containing and directing the energy of the expanding steam, thus helping to optimize the destructive work potential of the explosion.

In the BORAX tests, self-limiting power excursions were performed with exponential periods ranging between ~ 100 and 5 ms at boiling temperatures and between 100 and 13 ms at ambient temperatures. Minor damage to the core occurred during these tests, but the results indicated that shorter periods with larger energy releases could lead to extensive core damage. The BORAX program was completed with a 2.6-ms test, yielding a maximum power of 19 GW and a burst of energy of 135 MJ. This test destroyed most of the core and partially destroyed the facility. The SPERT-I tests also concluded with destructive loadings on the core and facility buildings. In the SPERT destructive test, $\sim 3.5\%$ reactivity insertion with a period of 3.2 ms caused gross core melting, releasing ~ 41 MJ total nuclear energy (peak power of 2.3 GW), with ~ 4 MJ of additional energy released from the aluminum-water chemical reaction.

Note that destructive steam explosions did not occur in the SPERT-II test series conducted with a D_2O -moderated core. The prompt critical excursions of this test series were not severe enough to cause rapidly superheated aluminum fuel (molten) mixtures in contact with water as obtained in the SPERT-ID test. Test 26 in the SPERT-II series led to power excursions beyond departure from nucleate boiling (DNB),

resulting in partial melting in some of the plates. It was surmised that significant power oscillations with large amounts of undershooting permitted transfer of sufficient amounts of stored energy from the plates to the coolant and helped prevent a violent steam explosion from occurring.

It was believed that the SL-1 incident was initiated by an insertion of $\sim 2.4\% \Delta k/k$ (3.4%) with a period of ~ 3.5 ms, causing gross core melting and superheating and releasing ~ 130 MJ of nuclear energy (total). Additionally, ~ 50 MJ was released by the melt-water chemical reaction. The expansion phase ejected the shield plug and raised the entire reactor pressure vessel 3 m from its supports, striking the elevated crane drive shaft above before falling back. Three operator fatalities resulted from this incident.

2.2 OUT-OF-REACTOR EXPERIMENTS

In the previously mentioned reactor tests, steam explosions occurred while the fuel geometry was essentially intact. All of the necessary conditions for a propagating steam explosion were satisfied (i.e., a well-mixed state, rapid energy deposition that caused high-temperature molten aluminum fuel, and the presence of a liquid slug for missile generation). This situation has no parallel in the commercial LWR area, where steam explosions are postulated to occur as shown schematically in Fig. 1. Here, following complete failure of

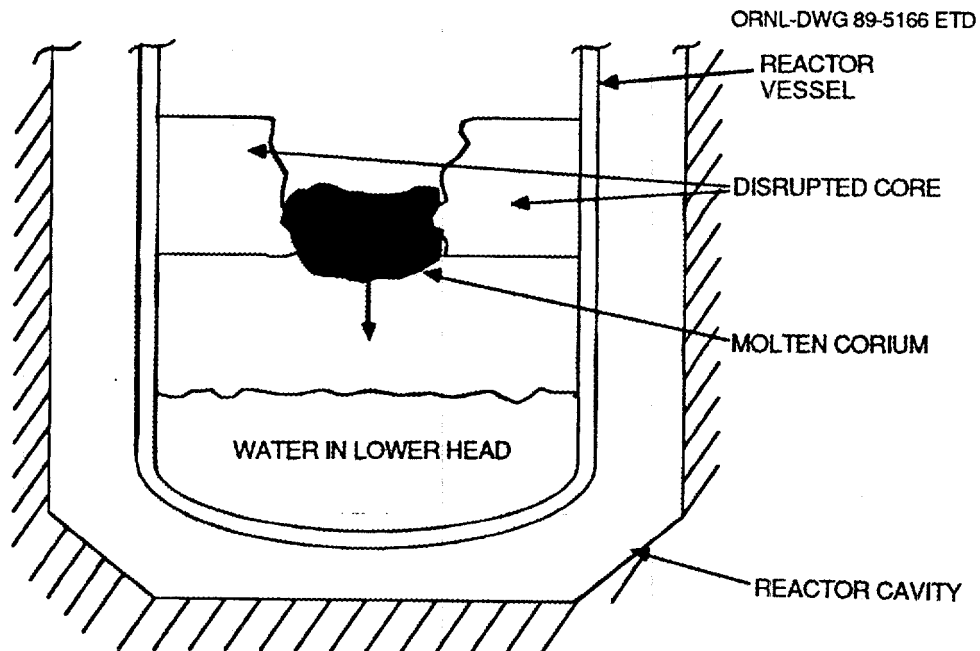
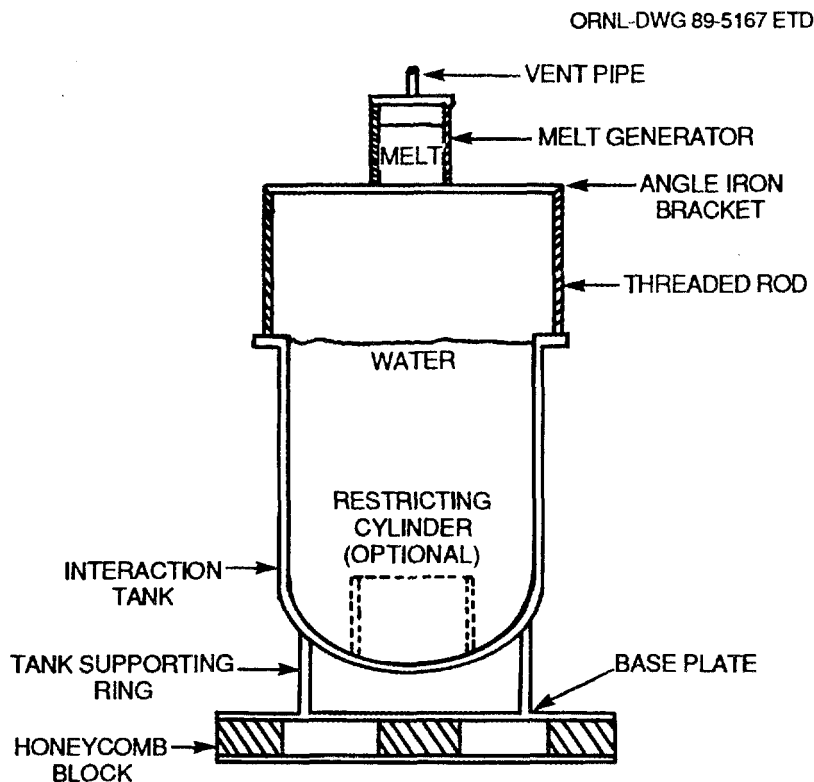


Fig. 1. Postulated steam-explosion scenario for commercial LWRs.

normal and emergency coolant flow, fission-product decay eventually causes melting of reactor fuel and cladding. This high-temperature molten corium mass can then interact with coolant in the lower plenum, causing steam explosions. Hence, all out-of-reactor experiments surveyed have involved simulation of the process shown in Fig. 1. Note that results from these experiments, along with insights gained from them, are also directly applicable to understanding steam-explosion characteristics for ANS. The reason is that steam-explosion phenomena in the ANS reactor will be analyzed from the standpoint of being initiated by reactivity excursions (with intact fuel geometry), as in the SPERT and BORAX tests, and also from interactions of high-temperature molten fuel falling into a pool of water, as shown in Fig. 1, or for ex-vessel explosions.

A good description of steam-explosion experimental analyses (non-reactor) has been given by Corradini.^{9,10} Nelson and Buxton¹¹ performed >300 small-scale experiments by using an arc-melter apparatus. Molten materials tested were stainless steel, Corium-A, Corium-E (see glossary), and iron oxide. Nelson et al.¹² have also conducted single-droplet experiments. Both spontaneous and triggered explosions occurred. Large-scale (5- to 20-kg fuel mass) experiments were originally conducted by Buxton and Benedick¹³ in an open chamber (Fig. 2)



using an iron-aluminum oxide fuel simulant. Most of the tests resulted in spontaneous steam explosions. Salient features are given in Table 2. As noted, Corium-A-related steam explosions had to be triggered by high energies. Analyses suggest this is because the initial temperature of the molten mass (~2800 K) is also approximately the liquidus temperature for Corium-A. Cooling analyses suggest that the melt could have cooled substantially in its fall through the air and water before an external trigger was fired to induce an interaction.

Table 2. Open geometry experimental observations⁴⁻⁶

Conversion ratio

The explosion conversion ratio with Fe-Al₂O₃ was between 0.2 and 1.4%.

Water temperature had little effect on the conversion ratio.

No energetic explosions with Corium-A+R (see glossary) were observed, a maximum conversion ratio was <0.05% using a large detonating cord trigger [-6 g of Pentonite (PETN) explosive].

Parametric effects

No obvious pour-rate effect was observed.

No interaction-volume effect was observed.

Possible melt quantity effect was observed.

Definite water-quantity effect was observed; as the mass of water increased, the conversion ratio increased.

Pressures

High, narrow pressure spikes were possible (20 MPa, <1 ms); 5- to 10-MPa sustained pressures were possible in large explosions.

Triggering

Spontaneous explosions were observed only for the Fe-Al₂O₃ melt and seemed to involve solid surface contact.

Artificial triggers (0.6 g of PETN explosive) were used for the Fe-Al₂O₃ melt, but did not modify the conversion ratio.

Only when the trigger magnitude was substantially increased did a small explosion occur with Corium-A+R.

Debris

Debris was similar to that observed in small-scale arc-melter experiments for the Fe-Al₂O₃ fuel melt.

The second large-scale experimental series has been conducted by Mitchell¹¹ and referred to as the fully instrumental test series (FITS). Salient features are outlined in Table 3. Note that the steam explosions were spontaneous and exhibited explosion-conversion ratios of 2 to 3% and pressure spikes of ~20 MPa for ~1 ms. More recently,¹⁴ the numbers related to the conversion ratio are considered to be ~10%. Also, unlike previous tests, the FITS experiments showed that violent steam explosions can indeed be generated under high ambient pressure surroundings although an external trigger was found to be necessary.

The aluminum industry has conducted hundreds of aluminum-water steam explosion experiments¹⁵⁻¹⁹ over several decades. Most of these

Table 3. FITS experimental observations⁹

Conversion ratio

The explosion conversion ratio with Fe-Al₂O₃ is consistently near 2 to 3%.

Pressures

High, narrow pressure spikes are always observed (~20 MPa for ~1 ms).

Lower sustained pressures follow behind this peak.

Propagation behavior

The fuel coarsely intermixes with the coolant before the interaction (time ~0.2 s).

A spontaneous explosion begins near the chamber base.

A detonationlike explosion wave is observed.

The explosion velocity varies between 200 and 600 m/s.

Initial conditions

As the fuel entry velocity is increased (>6 m/s) or the fuel mass decreased (≤2 kg), spontaneous explosions are suppressed.

Debris

The weight-averaged mean particle size after the explosion is ~150 to 250 μm and without an explosion is ~1 to 3 mm.

High-ambient pressure

A violent explosion was produced at an ambient pressure of 1.1 MPa by using an artificial trigger. The trigger was a detonator similar to that used in the open-geometry tests (0.6 g of PETN explosive).

experiments simulated a situation similar to that shown in Fig. 1, where molten masses of aluminum were dropped into a pool of water. The masses of aluminum poured ranged from 5 to 23 kg. Most of these experiments, which were performed without the use of artificial triggers, evaluated the effects of various coatings on the base of the container as well as the effect of key parametric variations (i.e., melt superheat, diameter of melt stream, and water depth). The likelihood of spontaneous explosion occurrence was qualitatively determined to rise with increasing melt superheat and melt-stream diameter. Again, spontaneous explosions did not occur if the melt had to travel more than ~0.76 m in the water before reaching the base surface. At water depths of 0.05 m or less, molten aluminum was blown out of the container. The nature of the base surface played a predominant role in determining both the likelihood and the intensity of the resulting steam explosions. In general, it was found that coatings of materials such as lime, gypsum, rust, or a sludge of aluminum hydroxide greatly increased the likelihood and violence of steam explosions, whereas coatings of materials such as grease or certain paints on the inside surface of the container prevented spontaneous explosions. However, later work¹⁸ showed that even inert surfaces could become active in the presence of sufficiently high trigger energy levels. The intensity of explosions ranged from moderate (i.e., the container remained intact) to very violent (i.e., the entire experimental setup was destroyed). The violent explosions involved chemical reactions of the molten aluminum with material at the base of the container. In these instances, the reaction-zone temperatures rose rapidly to well beyond the ignition temperature of aluminum.

Molten aluminum-water steam-explosion experiments have also been conducted by Fry et al.²⁰ at Winfrith, United Kingdom. Steam explosions were initiated using external triggers. The operating conditions were similar to those that can be expected in ANS. These experiments were thus used for benchmarking purposes and will be discussed again in Sect. 3.5.

Recently, Nelson²¹ conducted small-scale (i.e., using gram quantities of molten Al-6061) aluminum-water steam-explosion experiments that were supported by the Aluminum Association. Steam explosions were initiated through the use of artificial triggers. Nelson characterized the initiating mechanism for steam-explosion occurrence at contact surfaces based on the concept of wettability (i.e., the capacity to entrap a thin water layer between the solid surface and the molten material). Steam explosions were postulated to initiate from the rapid vaporization of a thin water layer between the melt and solid surfaces. This vaporization fragments the melt further, thereby leading to a propagating steam explosion. Based on previous experiments and analyses, Nelson also noted²² that if aluminum is mixed with other sensitive materials (e.g., lithium or copper), the characteristics can change radically such that spontaneous explosions always occur. Some aluminum alloys¹⁸ (e.g., Al-2011) are more prone to explosions than others (e.g., Al-PI520). Notably, Nelson's droplet experiments conducted with molten Al-6061 required a trigger pulse of ~2 MPa for initiation of steam explosions.

No information now exists, however, on the propensity of molten U_3Si_2/Al mixtures to undergo spontaneous explosions with water.

The Savannah River Laboratory (SRL)²³ is now also in the process of sponsoring several small- and large-scale steam explosion experiments at the Sandia National Laboratories (SNL), as well as separate effects tests at Rice University.

In summary, those experimental programs indicate the possibility and magnitude of destructive pressure pulses and energy conversions following metal-water steam explosions. In particular, they indicate the propensity for molten aluminum and its oxide to undergo spontaneous and/or triggered interactions with water when in contact with a wettable surface. The survey of the open literature experimental data base also indicated a strong dependence on the composition of the molten mixture for the initiation of steam explosions. Finally, the propensity for molten U_3Si_2/Al mixtures to undergo spontaneous steam explosions with water is now unknown.

3. CONVENTIONAL STEAM-EXPLOSION ANALYSIS FOR LWRs

The purpose of this chapter is to outline briefly the analytical framework developed for understanding steam-explosion phenomena. In particular, a mathematical model capable of giving reasonable estimates for pressure pulses is described and benchmarked. This model is then used in Chap. 4 for initial scoping studies for ANS.

As mentioned in Chap. 1, steam explosions evolve in four stages: (1) fuel-coolant mixing, (2) triggering, (3) explosion propagation, and (4) expansion. These are all complex phases because several unknowns are involved (e.g., molten fraction available, thermodynamic properties and distribution of the melt, and structural configuration during a meltdown accident). Several attempts have been made to quantify these stages by various researchers. These approaches are described below.

3.1 FUEL-COOLANT MIXING

Intimate fuel-coolant mixing is considered necessary to generate the large contact areas necessary for rapid heat transfer. As mentioned in Chap. 1, this criterion was already met for the destructive reactor tests.²⁻⁵ A similar case can be made for ANS. However, barring such incidents, once the core melt has entered the water (Fig. 1), it slowly breaks up and mixes with the water. One important parameter is the maximum quantity of melt that can intermix with the coolant before an interaction occurs or the melt solidifies. This parameter gives an upper bound on the explosion work potential. Several models^{14,24-26} have been proposed by Corradini, Henry, Theofanous, Fauske, Cho, and others, but they are all somewhat crude, requiring assumptions that lead to conservative or nonconservative results. Corradini observed²⁷ that in the FITS experiments (Fig. 3), the melt (5 kg) rapidly mixes with a large fraction of water (50 kg) before explosion occurs. He surmised that not more than 10 to 20% of the core in a commercial pressurized-water reactor would mix with water in the lower plenum before an explosion occurs.

Interesting and useful insights can also be obtained from Figs. 4 and 5, which show explosion conversion ratio and debris diameter as a function of coolant-to-fuel-mass/volume ratios. As seen therein, the conversion ratio for expected molten masses/volumes is relatively constant. The general subject of mixing is highly complex and is the subject of considerable debate in the commercial LWR industry.

3.2 TRIGGERING

Triggering can occur either spontaneously by the contact of molten masses with structures or by external detonators. Although impact forces and pulses from detonators are easy to evaluate, spontaneous triggers are difficult to model because their causes are not well-known.

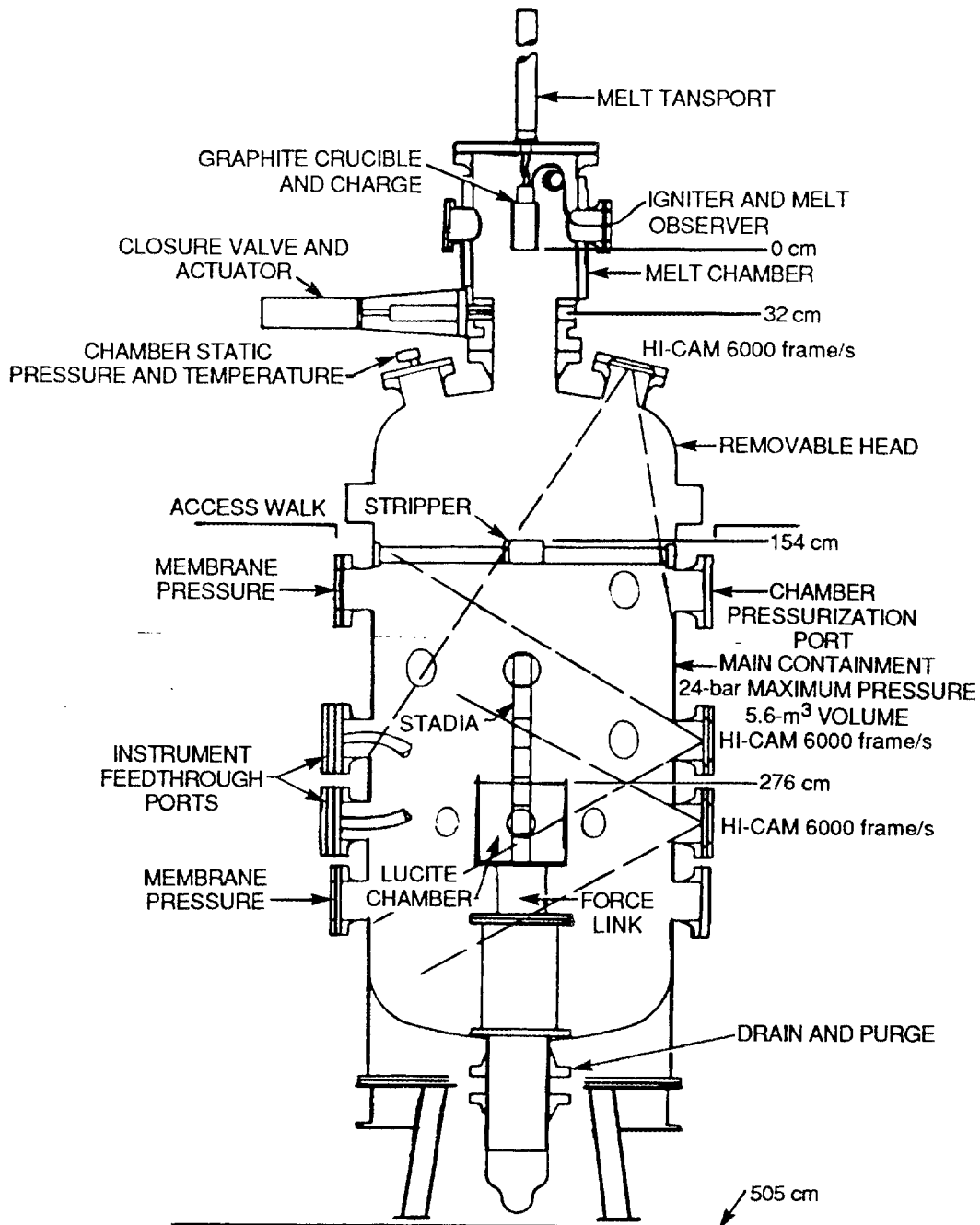


Fig. 3. Schematic representation of FITS experimental setup (Ref. 11).

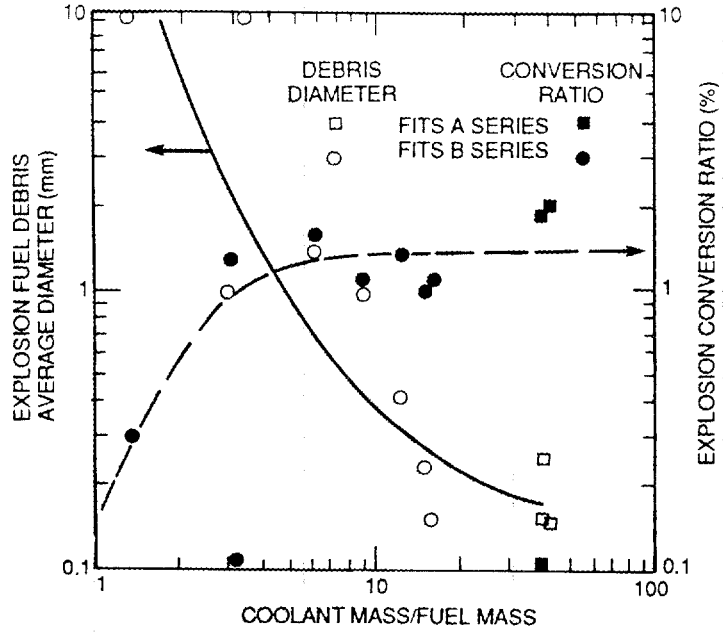


Fig. 4. Explosion-conversion ratio and debris diameter as function of coolant-to-mass ratio (Ref. 9).

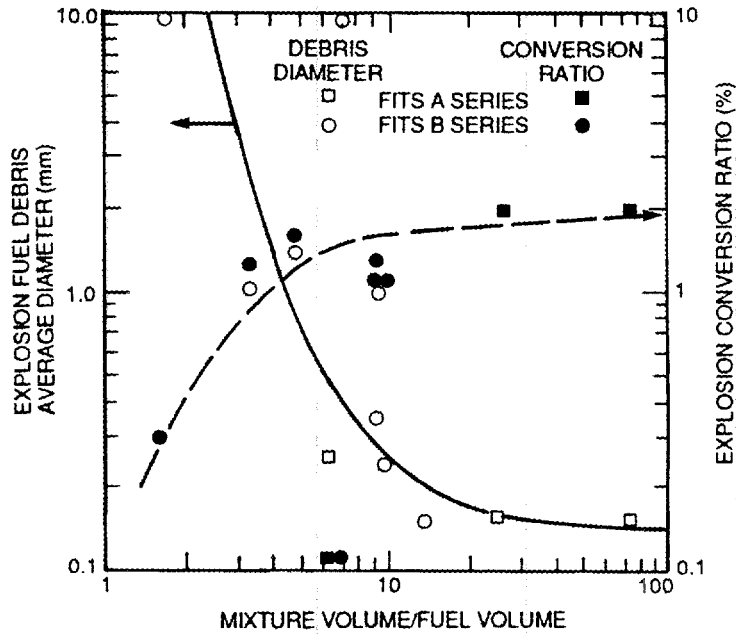


Fig. 5. Explosion-conversion ratio and debris diameter as function of mixture-to-fuel volume ratio (Ref. 9).

Most of the FITS experiments conducted with aluminum oxide and large-scale experiments conducted by the aluminum industry¹⁵⁻¹⁹ exhibited spontaneous explosions. It is also known that molten aluminum when mixed with certain materials (e.g., lithium or copper) explodes spontaneously upon interacting with water. Thus, it seems prudent to assume that in the absence of U_3Si_2/Al fuel-coolant interaction data for ANS steam-explosion studies, sufficient trigger energies would exist for a propagating fuel-coolant interaction to occur.

3.3 PROPAGATION

This phase represents the early time domain (typically 0.1 to 10 ms) after the steam explosion, during which significant pressure pulses are generated. Several mechanistic and empirical models have been proposed over the past several years with varying degrees of success. The so-called Integrated Fuel Coolant Interaction Code²⁸ (IFCI) is a state-of-the-art mechanistic modeling program under development at SNL. Corradini modeled one-dimensional (1-D) aspects of Mitchell's experiments using his 1-D mechanistic model.⁹ A key ingredient in these mechanistic models deals with the fuel-fragmentation scheme that initiates and sustains the explosion. Various models have been proposed. See Refs. 9, 14, 24, and 28 for additional information.

An alternative to mechanistic modeling that provides good estimates for the propagation phase has been given by Corradini.⁹ It consists of using an empirical steam-explosion model with a two-dimensional (2-D) hydrodynamics code, CSQ.²⁹ Besides the relative simplicity of modeling, it also simulates 2-D effects. In the FITS experiments, the explosion exhibited multidimensional characteristics that can cause a nonuniform pressure loading on the surrounding structure and can mitigate the explosive work potential compared with that predicted by a 1-D analysis. Hence, the empirical model can be expected to provide a more realistic picture. This model is based on the physical concept that the fuel melt and the coolant in the explosion zone interact and come to thermal equilibrium before substantial coolant expansion occurs. Figure 6 shows a simulation of a FITS experiment using the empirical model with the CSQ wave code. As shown, the model predicts the pressure pulse and duration with good accuracy.

A containment failure study²⁷ conducted by Corradini also used this approach. The ratios of coolant-to-fuel masses interacting were taken as 1/16 (conservative, Case 2), and 1/1 (best estimate, Case 1). Figure 7 shows the essential aspects of the analyses. As noted, Case 1 results in characteristic peak pressures and pulse durations of ~100 MPa and 1 ms, respectively. Case 2 results lead to peak pressures and pulse durations of ~400 MPa and 2 ms. These pressure-time histories were next used in a transient calculation to evaluate failure of the reactor vessel lower plenum. Failure analysis is described later in Sect. 3.5.

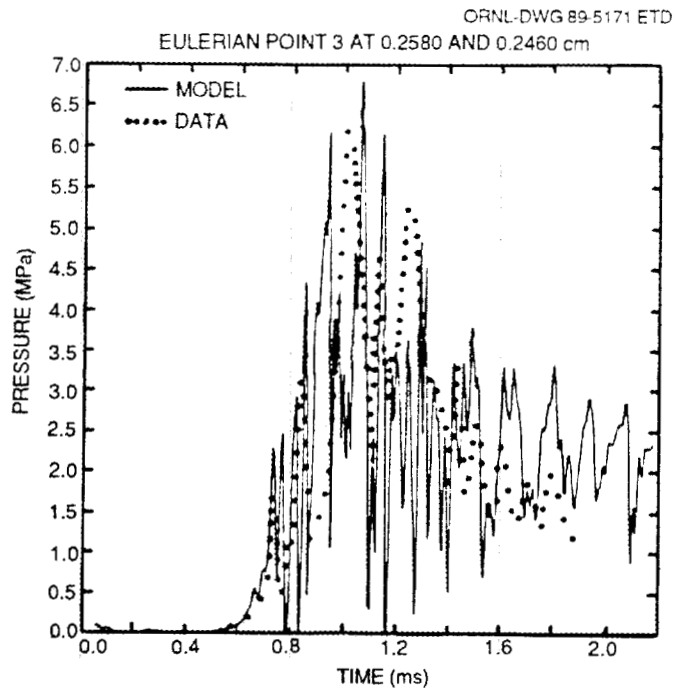


Fig. 6. Comparison of calculation and data for FITS test MD-19 (Ref. 9).

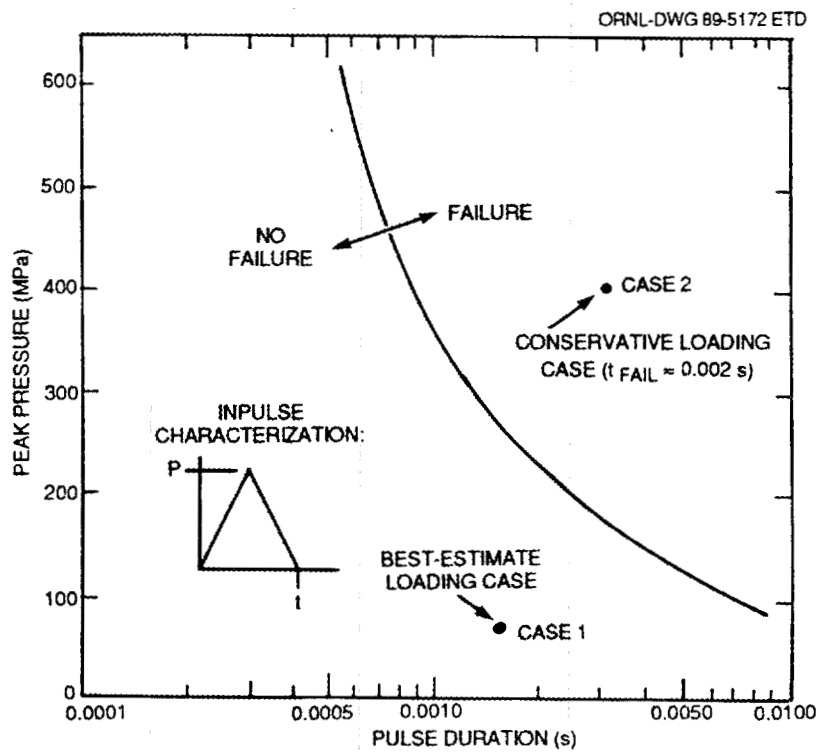


Fig. 7. Failure envelope for lower plenum under initial pressure-pulse loading immediately after steam explosion, cases 1 and 2 (Ref. 27).

3.4 EXPANSION

Expansion represents the later phase of the transient (i.e., >10 ms). After the explosion has been triggered and has propagated through the melt-coolant mixture, the resulting high-pressure steam expands and does work against its surroundings. This work can be destructive. The three basic methods for estimating the expansion work potential are (1) thermodynamic expansion model,³⁰ (2) 1-D expansion model,³¹ and (3) 2-D expansion model.²⁷

The thermodynamic expansion model is the most conservative, giving energy conversion ratios in the range of 20 to 30%, far above what has normally been observed experimentally. This approach represents upper-bound calculations and is not recommended for realistic (i.e., best-estimate) studies.

In the 1-D model, a lumped parameter approach that allows for mechanistic heat-transfer models was used to represent the explosion expansion as a two-phase high-pressure coolant mixture accelerating a voidless rigid water slug (Fig. 8). It allows for water entrainment

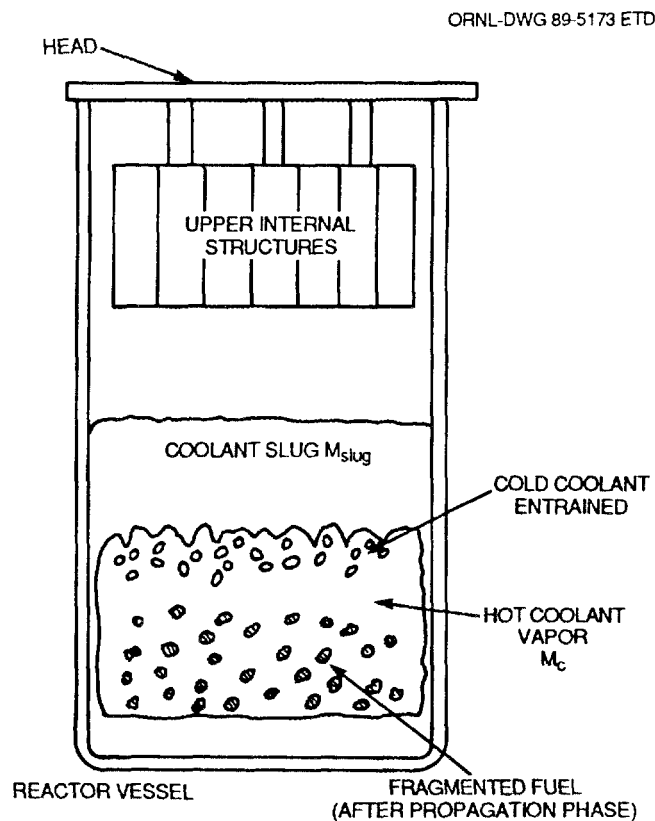


Fig. 8. Schematic representation for 1-D expansion model (Ref. 27).

during expansion and quenching of high-pressure steam. This approach gives conversion ratios 2 to 5 times lower than the thermodynamic model, bringing it close to experimental observations.

The 2-D model was used by Corradini²⁷ with CSQ, along with the empirical steam-explosion model described earlier. It is superior to the 1-D model because effects such as liquid slug deformation and breakup can be accounted for. Such a slug deformation was also noted by Los Alamos investigators.²⁹

3.5 FAILURE ANALYSIS

As mentioned earlier, upon steam-explosion occurrence, the high-pressure steam expands and does work on its surroundings. Traditionally,²⁷ analyses evaluate loadings in two stages, as follows.

3.5.1 Response to Initial Pressure Pulse

The first stage consists of evaluating the impact of high-pressure pulses immediately following (≤ 5 ms) a steam explosion. In the study reported in Ref. 27, a 1-D model was developed to set up a failure envelope for the lower head of the LWR pressure vessel. Spherical geometry was assumed along with elastic-plastic material response. Specifically, the model solved the following dynamic equation:

$$\ddot{w} = \frac{pR - 2t\sigma}{Rt\rho} , \quad (3.1)$$

where,

t = thickness,
 R = radius,
 σ = stress,
 ρ = density,
 p = pressure,
 w = radial displacement.

The failure criterion used in this case was based on a comparison of calculated effective plastic strain to uniaxial strain of fracture. Using data from Ref. 32, the criterion used was

$$\frac{\epsilon_{\text{uniaxial}}}{\epsilon_{\text{biaxial}}} = 2.25 , \quad (3.2)$$

where ϵ denotes strain.

Solving Eq. (3.1) with that failure criterion, the study generated a failure envelope as shown in Fig. 7 for the so-called best-estimate

and conservative cases, respectively. As noted in Fig. 7, the best-estimate case indicates no failure, whereas the conservative case leads to failure of the lower plenum.

3.5.2 Response to Slug Loading

During the second stage, a slug consisting of solid debris, liquid, and vapor accelerates and comes into contact with the upper boundary of the reactor vessel. In the study given in Ref. 27, a 1-D (finite-element) representation was used for evaluating slug impact with the upper head. In this case, the failure assessment was based on fracture mechanisms for various key components (e.g., studs and closure head), using stress-intensity factors. The structural model used is shown in Fig. 9 and was developed using the HONDO-II Code.³³

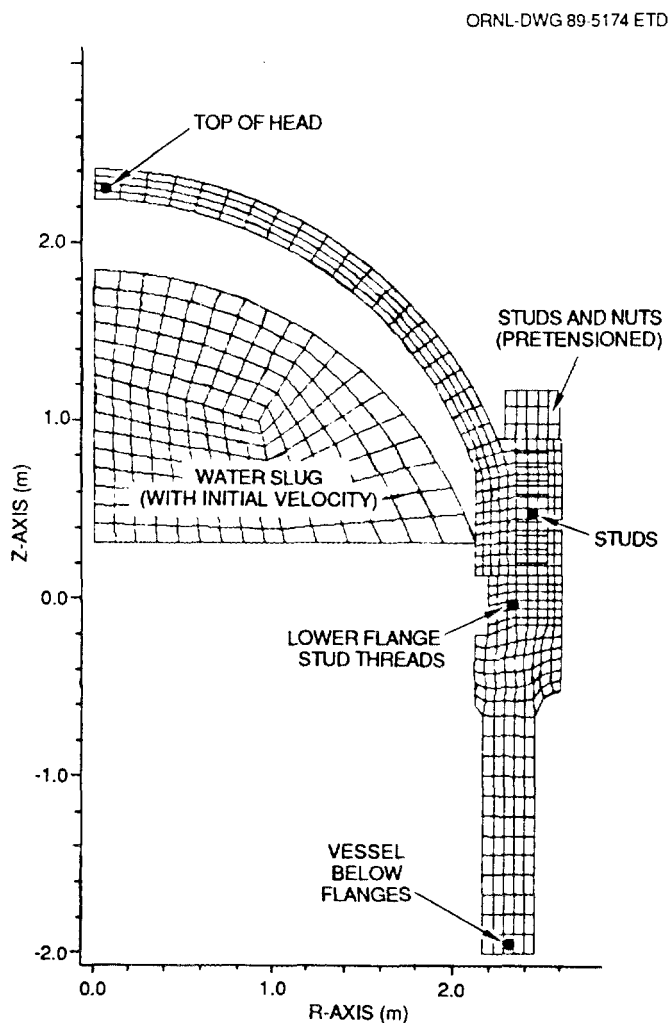


Fig. 9. Structural model and locations of failure for LWR steam-explosion-related failure evaluation (Ref. 27). Boxed items have been evaluated for failure.

Considerable uncertainty exists concerning the slug-energy content.¹⁴ For the sake of illustration, Ref. 27 values are given here in considering three cases. The first, considered realistic, assumes that 10% of the PWR core interacts with 10,000 kg of water with a conversion ratio of 1%, leading to 300 MJ of expansion work and a 12,500 kg slug with a velocity of 200 m/s. The conservative case assumes that 40% of the core mixes with 20,000 kg of water and undergoes an isentropic coolant expansion, leading to 3000-MJ expansion work and giving rise to a 12,500-kg slug with a velocity of 690 m/s. In the third case, values were taken from a Los Alamos study¹² using SIMMER. In this instance, 20% of the core was assumed to participate. The coolant-to-fuel-mass ratio was 1/16, giving rise to a peak kinetic energy of 1200 MJ. The three different loading mechanisms shown in Fig. 10 are (1) coherent water slug impact, (2) pressure/time history on reactor vessel defined by SIMMER calculations, and (3) upper-core support plate (UCSP) impact with the vessel head.

The results of these calculations are summarized in Table 4. As noted, the top of the head is predicted to fail first for all loading conditions where failure is expected, and the kinetic energy of the head at failure is given.

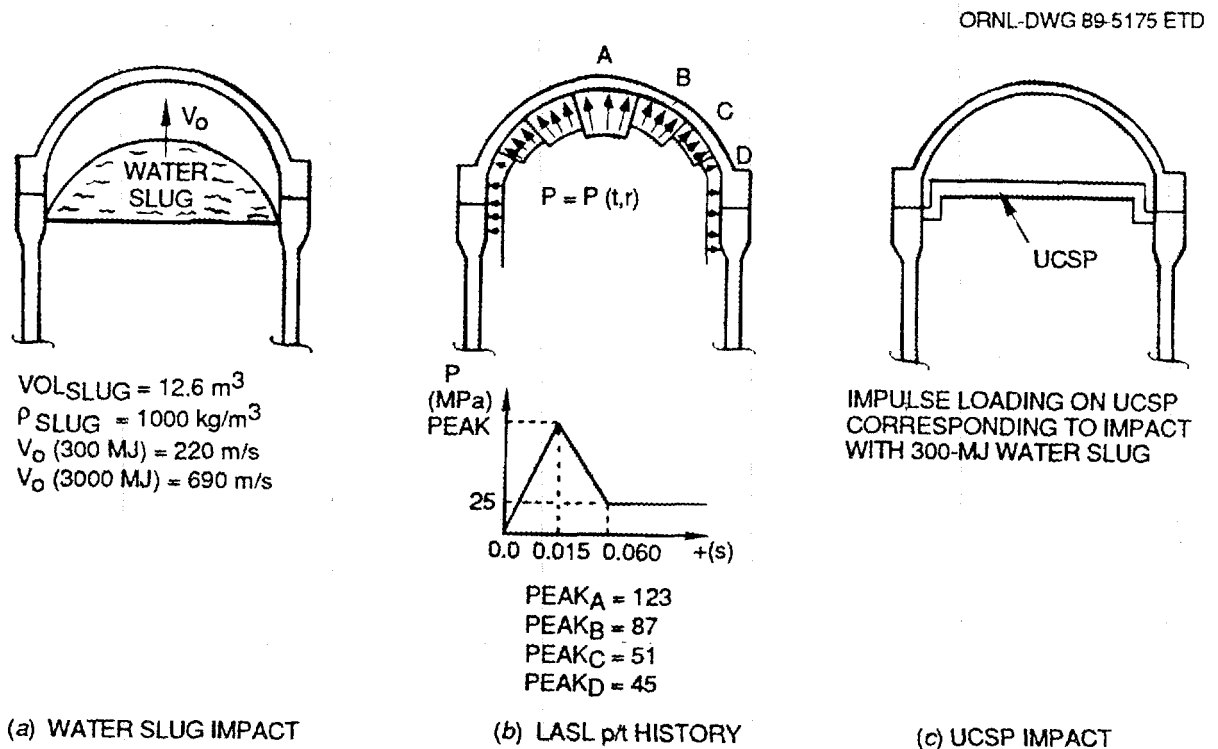


Fig. 10. Steam-explosion loading mechanisms for expansion phase of steam-explosion transient (Ref. 27).

Table 4. Summary of commercial LWR
vessel-failure evaluation²⁷

Case	Failure at top of head	Failure at stud	Failure at vessel below flanges
300 MJ	Yes	Yes	No
3000 MJ	Yes	Yes	No
Los Alamos Scientific Laboratory p/t history	Yes	No	No
Upper-core support plate		No	No

3.5.3 Missile Generation

If the upper head of the RPV were to fail, missiles could be generated that might cause the containment to fail. The type of missiles generated and consequences thereof are highly dependent on the geometrical setup and operating conditions. Various empirical correlations³⁴⁻³⁶ have been documented in the literature for penetration of concrete by missiles. These equations, generally speaking, tend to be conservative. Another (albeit more expensive) approach uses a sophisticated wave code, as was done in Ref. 27, for obtaining improved estimates of concrete penetration.

3.5.4 Ex-Vessel Steam Explosions

The analyses described above dealt with in-vessel steam explosions. However, it is conceivable that on melting the lower plenum vessel wall, molten fuel could encounter water in the reactor cavity.

The result could be an ex-vessel steam explosion. The consequences of such an explosion are highly dependent on the operating conditions and reactor/containment design. A properly designed cavity would tend to retain effects of the explosion and prevent the containment from leaking. Care should be taken to avoid efficient coupling of the steam-explosion energy with solid material to prevent missile generation.

3.6 PROBABILITY OF CONTAINMENT FAILURE

Based on the analytical framework presented in this section, estimates can be obtained for the probability of containment failure. As

noted earlier, the phenomena being analyzed are quite complex, consisting of stochastic and deterministic processes. Hence, engineering judgment is sometimes required to evaluate the probability of containment failure. WASH-1400 (Ref. 1) used the formula

$$P_{\alpha} = P_{fcc} P_f P_c, \quad (3.3)$$

where

- P_{α} = probability of containment failure resulting from steam explosion,
- P_{fcc} = probability of water being present in the lower plenum when a major fraction of the core is molten ($\geq 20\%$),
- P_f = probability of FCIs after fuel-coolant contact resulting in fuel fragments < 5 mm,
- P_c = probability/fraction of steam explosions leading to containment failure.

WASH-1400 (Ref. 1) estimated the values of P_{fcc} , P_f , and P_c as 1, 0.1, and 0.1, respectively, leading to a value of 0.01 for P_{α} . In a later study,²⁷ the lower and upper bounds of 0.0001 and 0.01 were estimated for P_{α} . The lower bound represents so-called best estimate calculations, whereas conservative estimates gave the upper bound.

Note that Eq. (3.3) would need to be implemented differently for differing reactor and containment designs, especially for the ANS design applications. For example, P_{fcc} would need to include the possibility of steam explosions resulting from power excursions, similar to the SPERT-1 (Ref. 3) and similar tests. A systematic study would identify such differences to characterize overall system-dependent dynamics correctly.

A so-called new probability of containments-failure approach, which represents a major technological advancement, has been developed by Theofanous et al.,¹⁴ under Nuclear Regulatory Commission (NRC) sponsorship. This structured approach was applied by the authors for a specific set of conditions (i.e., pressurized-water reactor and low pressure), along with assumptions for key events in the overall process, for setting probability distribution functions. The result indicated low containment-failure probability. However, the authors have been careful to stress the subjectivity aspect and have shown that small changes in key parameters can change the probability of containment failure by several orders of magnitude to indicate definite failure, as shown in Fig. 11. Hence, caution is advised when transferring results from one scenario to another.

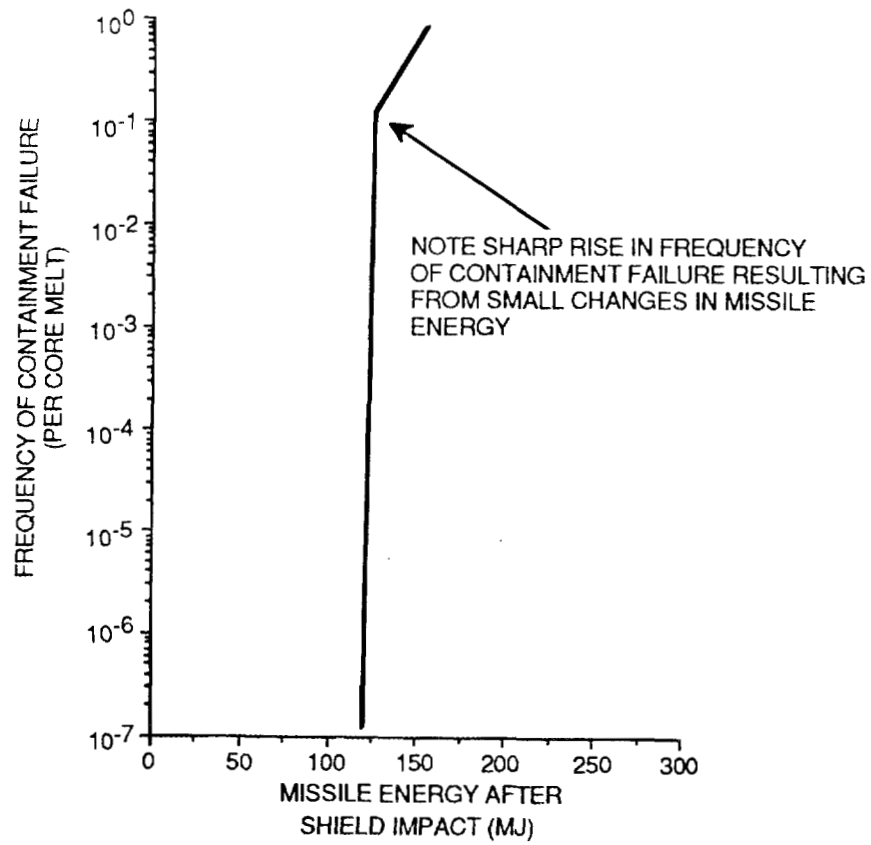


Fig. 11. Frequency of containment failure vs missile energy for LWR analysis (Ref. 14).

4. MODELING AND BENCHMARKING FOR ANS STUDY

As described in Sect. 3, steam-explosion analysis can be separated for convenience into two phases. The first phase deals with evaluation of the initial pressure pulse immediately (typically ≤ 5 ms) following a steam explosion. The physically based empirical model given by Corradini⁹ can be used to obtain estimates for peak pressure-pulse magnitudes. Note that the actual modeling of pulse evolution would require using wave codes. However, it has been seen experimentally that pressure-pulse durations lie in the 1-ms range. Hence, from an engineering standpoint, we will assume the pulse duration to be 1 ms. The impact of this assumption can be qualitatively evaluated once the relevant failure envelope has been generated, as was done in Chap. 3 (Fig. 7).

The simple model is implemented in two steps. In the first step, an equilibrium temperature is evaluated for the fluid from this equation:

$$T_e = \frac{T_f + [(mC)_c / (mC)_f] T_c}{1 + [(mC)_c / (mC)_f]}, \quad (4.1)$$

where

m = mass,
 c = specific heat,
 c, f = subscripts denoting coolant and fuel, respectively.

In the second step, the temperature T_e is introduced in the Redlick-Kwong equation of state given by

$$P_e = \frac{RT_e}{(V_e - a_r)} - \frac{b_r}{[T_e^{1/2} V_e (V_e + a_r)]}, \quad (4.2)$$

where

p = pressure,
 R = gas constant for water,
 V_e = equilibrium two-phase specific volume (i.e., reciprocal of the two-phase mixture density),
 a_r, b_r = 0.00117 and 43,961, respectively.

Before applying this model directly to the ANS reactor (Chap. 5), the model results were compared against an earlier calculation reported in Ref. 10. Details of this comparison are shown in Table 5. As noted, both sets of numbers are in good agreement even though a different equation of state was used for our calculations.

Table 5. Model verification calculations

Results	Present calculation ^a	Previous calculation ^b
Peak pressure (MPa)	109	~100
Operating conditions		
Fuel temperature = 2300 K		
Void fraction = 0.35		
Coolant temperature = 300 K		
Mass of coolant to = 1.0		
mass of fuel ratio		

^aCalculations using the Redlick-Kwong equation of state.

^bCalculations from Ref. 10 using the ANEOS and THEOS equations of state.

Next, the model given by Eqs. (4.1) and (4.2) was applied to predict the pressure-pulse magnitude noted in one of the aluminum-water steam-explosion experiments conducted (experiment T122) by Fry²⁰ at Winfrith, United Kingdom. Essential details are shown in Fig. 12. As shown therein, two sets of pressure gages denoted U (upper level) and L (lower level) were present for pressure-pulse detection. The U pressure gages detected pressure-pulse magnitudes of ~35 to 40 MPa, whereas the L gages recorded values of ~50 to 60 MPa. Molten aluminum was exploded close to the L gages. Hence, peak pressures at the explosion source can be roughly estimated as ~60 to 70 MPa. Results of a parametric study are shown in Table 6. As noted therein, the model gives estimates that are close to the experimental values.

The empirical model was next used to estimate the peak pressure pulse levels reached immediately following a steam explosion event in the SPERT-ID³ and SL-1⁴ reactor reactivity excursion-induced destructive incidents. In such reactors, with narrow fuel-to-coolant gaps between plates, small amounts of coolant mass vaporization can lead to large void fraction levels. It was estimated that the coolant void fraction would be in the 70% to 80% range. Based upon the volumes of fuel and coolant in the core, it was further estimated that the coolant-to-fuel mass ratio in the explosion zone would be about 0.5. Again, based upon the reported values of heat deposition, it was estimated that the maximum fuel temperature in each of these destructive incidents was at least 1700 K for the SPERT-ID test,³ and about 2400 K for the SL-1⁴ incident. With these values, the model described earlier gave estimates for peak pressure pulse levels (in the explosion zone) ranging from 67 to 97 MPa for the SPERT-ID test, and from 100 to 145 MPa for the SL-1 incident. In comparison, oscillations of +60 MPa were recorded by pressure transducers (located just outside the core) for the SPERT-ID test.³ It was estimated that the average peak steam pressure during the SL-1 incident⁴ was at least 75 MPa.

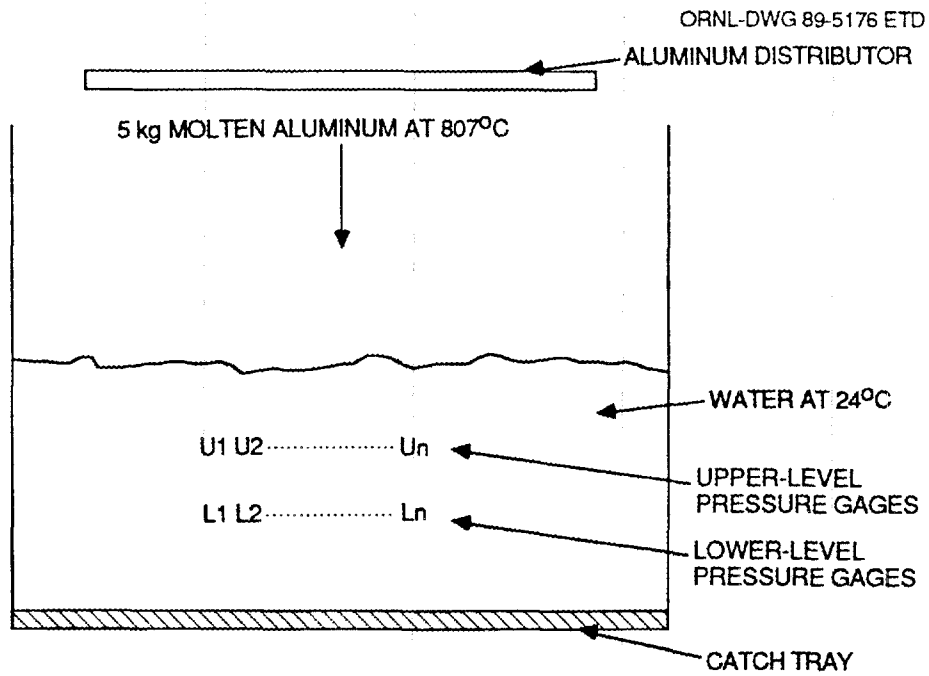


Fig. 12. Schematic representation of molten aluminum-water steam-explosion experiment T122 at Winfrith (Ref. 20).

Table 6. Model benchmarking calculations with experiments²⁰

Mass ^a fraction	Void coolant two-phase fraction	Peak pressure magnitude (MPa)
1.0	0.5	60
1.0	0.3	56
1.0	0.0	20
0.5	0.5	91
0.5	0.3	103

^aMass fraction is defined as the ratio of coolant mass to mass of fuel.

As seen, the evaluated pressure pulse magnitudes are in good agreement with test data; along with the previous experimental benchmarking results, they indicate the appropriateness of the modeling approach and methodology for evaluation of steam explosion-induced peak pressure pulse magnitudes for U-Al fueled, plate-type research or test reactors.

The later phase of the transient (≥ 10 ms) deals with the phenomenon of high-pressure steam expansion that does work against the surroundings, generating an energetic slug of water that could cause missiles to breach the containment. In this instance, the assumption will be that water is present. The major unknown is the energy-conversion ratio. Currently,¹⁴ the best estimate is ~10%, with significant uncertainties. Because of this, the estimated available thermodynamic energies evaluated in Appendix A will be used in Chap. 4 as the upper-bound conservative estimates. The equation used for generating slug velocities in the ideal sense is given by

$$v_{\text{slug}} = (2E/m_{\text{slug}})^{1/2} , \quad (4.3)$$

where

$$\begin{aligned} v_{\text{slug}} &= \text{slug velocity,} \\ E &= \text{available mechanical energy,} \\ m_{\text{slug}} &= \text{mass of slug.} \end{aligned}$$

Note that the velocities evaluated from Eq. (4.3) can be expected to give upper-bound values because the following simplifying assumptions were made in this report for evaluation of slug energetics:

1. Mechanical energy is transferred to the slug instantaneously. In reality, the mechanical energy would be transferred over a finite time period.
2. Compressibility effects are negligible. As the slug velocity approaches sonic levels, these effects become important. Note, however, that the sonic velocity in a liquid medium varies inversely with the square root of the material density, which further, is dependent on the local temperatures and pressures. Hence, the actual situation is more complicated than it might appear at first glance. In a good mechanistic analysis, the use of wave codes would consider these variations on sonic propagation, as well as initiation of shock waves, if the conditions so dictate.
3. Multidimensional effects are negligible. In reality, the slug energetics can be expected to be affected significantly by multidimensional effects, such as slug deformation and dissipation. Such phenomena would tend to reduce the destructive potential of material slugs.

For specific ANS applications where steam explosions may occur from reactivity excursions, the primary coolant system would not encompass a void space for slug acceleration (i.e., as thought of conventionally). In these cases, the mechanical energy imparted to the coolant would tend to cause the system pressure to rise because of coolant compression within fixed structural boundaries. If loop-pressurization levels exceed design ratings, failure can be expected, with consequent expulsion of coolant-material mixtures in the form of slugs or blowdown sources. The propagation of these slugs or blowdown sources, and the effects of slug and missile impact on structures, should be analyzed in the manner outlined previously.

The pressure rise in the loop caused by the mechanical energy of compression can be roughly estimated^{4,5} from Eq. (4.4), given as

$$\Delta P_{\text{rise}} = [2E_{\text{comp}} / (V\beta)]^{1/2} , \quad (4.4)$$

where

- ΔP_{rise} = loop fluid pressure rise,
- E_{comp} = mechanical energy of compression,
- V = volume of fluid,
- β = fluid compressibility.

5. PRELIMINARY STEAM-EXPLOSION ANALYSIS FOR ANS

5.1 ESTIMATED ANS EXPLOSION LOADINGS

The analytical framework developed in Sect. 4 was used next to evaluate the dynamics of steam-explosion phenomena as applied to the ANS core region. The numbers generated are intended to give "order-of-magnitude" estimates only for expected pressure pulses and slug energetics. Analyses are conducted in the following three stages.

Fuel and coolant properties are assumed to be the same as given in Appendix A of this report. Numerical values for the various parameters used are shown in Table 7.

A parametric study was conducted to evaluate peak-pressure magnitudes. The results of these calculations, along with a sample calculation, are shown in Figs. 13 and 14. The fuel-temperature range encompasses the expected magnitude for the three basic accident cases derived in Appendixes A and B [i.e., reactivity excursion without scram ($T_f = 1327$ K), inadequate cooling without scram ($T_f = 1684$ K),

Table 7. Initial conditions for preliminary ANS calculations

Scenario	Fuel temperature (K)	Available energy (MJ)		
		Thermodynamic evaluations ^a		Experimentally based ^b
		Upper bound (thermal)	Best estimate (mechanical)	Best estimate (mechanical)
Reactivity excursion without scram	1327	121	35.1	12.1
Inadequate cooling without scram	1684	166	53.1	16.6
Inadequate cooling on decay heat	873 ^c	64.5	17.1	6.45

Note: Coolant temperature was taken as 373 K for thermal-hydraulic evaluations.

^aValues of available energy obtained from thermodynamic calculations are presented in Appendixes A and B.

^bValues of available mechanical energy were obtained by multiplying the available (upper-bound) thermal energy by 0.1, which is now¹⁴ the experimentally based recommended value of the conversion ratio.

^cAssuming melt formation at 600°C (Appendix A).

ORNL-DWG 89-5178 ETD

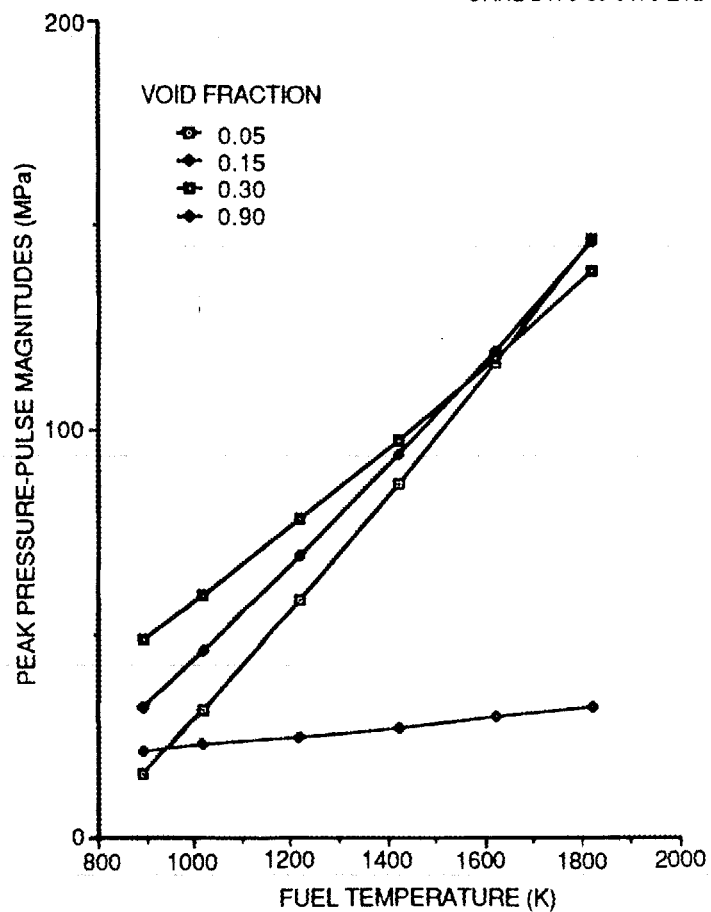


Fig. 13. Variation of peak pressure-pulse magnitudes vs fuel temperatures, coolant-to-fuel mass ratio = 1.0.

ORNL DWG 89 5179 ETD

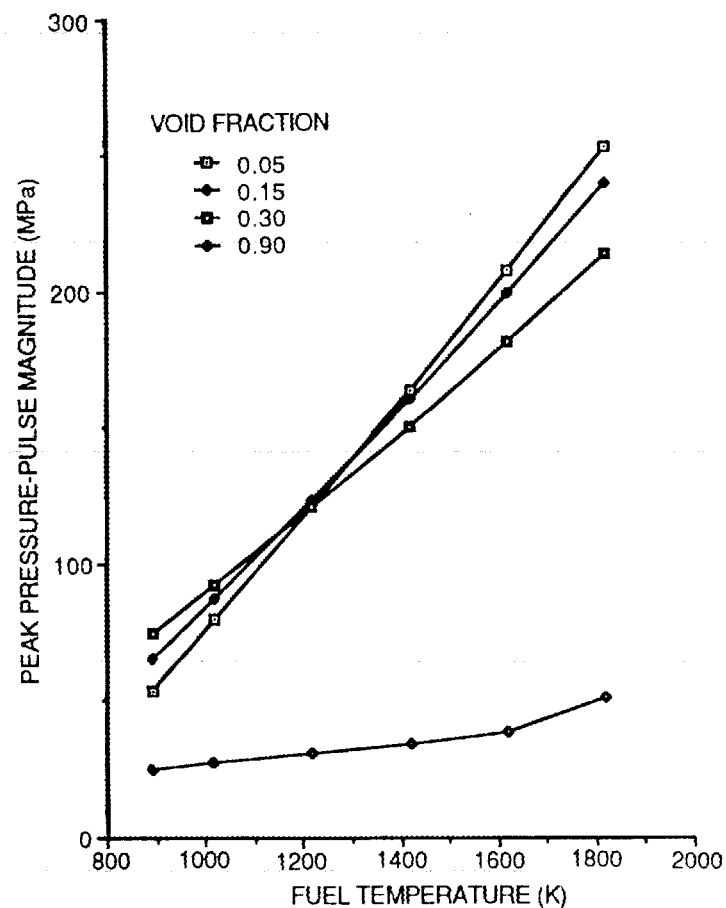


Fig. 14. Variation of peak pressure-pulse magnitudes vs fuel temperatures, coolant-to-fuel mass ratio = 0.5.

and inadequate cooling on decay heat ($T_f = 873$ K)]. As expected, peak-pressure magnitudes increase with rising fuel temperatures and exhibit a fairly strong dependence on void fraction and coolant-to-fuel mass ratio in the explosion zone.

Notably, these values are several orders of magnitude lower than those calculated previously,³⁷ where the explosive pressures were based on chemical detonation. For comparison, these values are also indicated in Table 8 against likely pressure-pulse magnitudes calculated using Eq. (3.2). Such a comparison clearly emphasizes the fundamental differences between steam explosions and chemical detonations referred to in Chap. 1.

Results of parametric calculations for slug energetics are displayed graphically in Fig. 15. As noted, the mechanical energy imparted to slug mixtures can give rise to very high velocities. These velocities were evaluated using Eq. (3.3) and are representative of a situation in which a void volume is present immediately adjacent to the explosion zone.

The pressure rise in the loop resulting from the mechanical energy of compression was evaluated using Eq. (3.4). The results of these evaluations at various energy levels and volumes of compression are displayed in Fig. 16. Such a pressurization can be expected in the event

Table 8. Comparison of pressure-pulse magnitudes from steam explosions with chemical detonations

Scenario	Peak pressure magnitude (MPa)			
	Present calculations ^a			Detonation calculations ³⁵
	$\alpha = 0.05^b$	$\alpha = 0.3$	$\alpha = 0.90$	
Reactivity excursion without scram	74	87.5	24	$\sim 10^3$
Inadequate cooling without scram	126	123	28	$\sim 10^3$
Inadequate cooling on decay heat	13.7	46.5	20	~ 700

Note: Values obtained from detonation calculations were taken from Ref. 37 via extrapolating curves of Fig. 2 to radius = 0.0 m (i.e., to the source of detonation).

^aAssuming a coolant-to-fuel mass ratio of 1.0 in the explosion zone.

^bVoid fraction of two-phase mixture.

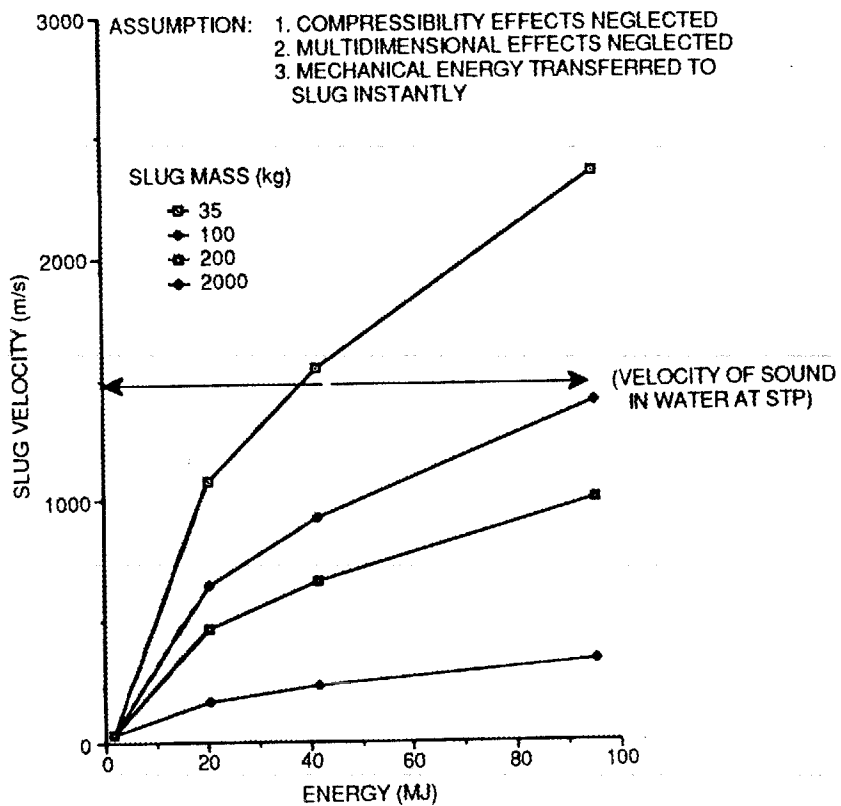


Fig. 15. ANS slug energetics during expansion phase.

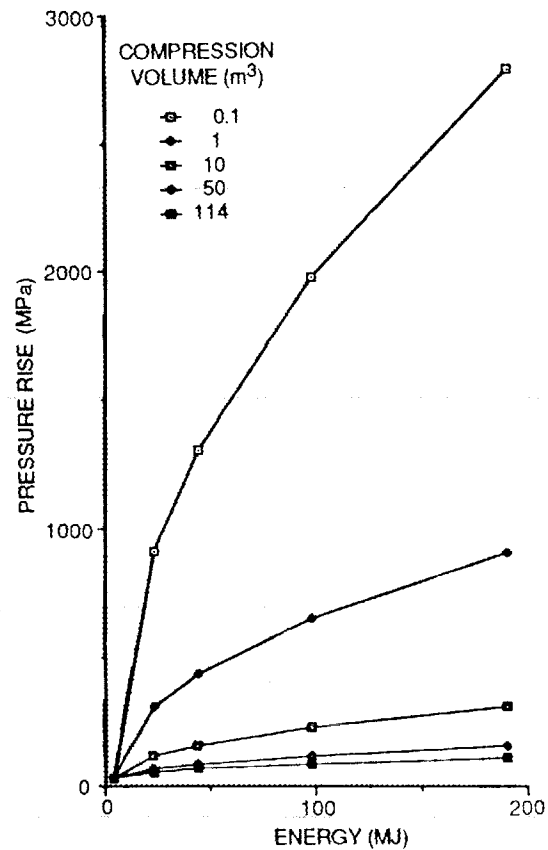


Fig. 16. RCS loop-pressurization parametrics.

of steam explosion in the core region with the loop completely filled with water. Note that the compression-volume range considered varies from 0.1 m³, approximately representing the core volume, to 114 m³, representing the entire RCS loop volumetric capacity.

5.2 ANS FAILURE ANALYSIS AND DESIGN IMPLICATIONS

As mentioned previously, a systematic failure analysis would involve either (1) setting up a failure envelope (as shown in Fig. 7) upon solving Eq. (3.4) or (2) using a finite-element code. Furthermore, evaluation of slug energetics, loop pressurization, and evolution of missiles upon interaction with vessel components would necessitate the use of techniques outlined in Sect. 3. Because of the preliminary nature of this study, detailed analyses have not been conducted. However, preliminary conclusions are provided, based on limited analyses and engineering judgment.

A failure envelope was generated by Gwaltney and Luttrell³⁸ for the core pressure boundary tube (CPBT) and reflector tanks subjected to triangular pressure pulses caused by a steam explosion in the core region. This failure envelope curve of peak pressure vs triangular pulse duration is shown in Fig. 17. The analysis included solutions of the elastic-plastic dynamics of a 2-D model of the CPBT and the reflector tank, as well as the D₂O held in the tank, which incorporates the effects of the tank's inertia and stiffness. Figure 17 was generated by modeling the system with the general-purpose finite-element code ADINA. The aluminum walls were assumed to be an elastic, perfectly plastic material with a yield stress of 241 MPa. Failure is assumed to occur when the tube becomes completely plastic throughout the thickness.

The structural response model did not account for the presence of other structural materials (e.g., beam-tube penetrations and cold source) that may also collapse from the pressure pulse, and in so doing, absorb some of the energy from a steam-explosion event. The model may thus be expected to give conservative estimates for pulse magnitudes that the reflector tank can withstand without failure.

As noted from Fig. 17, for pulse durations of ~1 ms, CPBT failure can be expected for pulse magnitudes >22 MPa. Indeed, for CPBT, this conclusion would hold true for pulse durations as low as 0.2 ms. The reflector tank can be expected to withstand pulse magnitudes as high as 75 MPa for 1 ms. For more energetic explosions with pressure pulses lasting longer than 10 ms, the reflector tank can be expected to withstand pulse magnitudes as high as 25 to 30 MPa.

As mentioned in Chap. 4, when evaluating the peak pressure pulse magnitudes, a key input parameter is the coolant void fraction in the explosion zone. For analyzing ANS steam explosions when the core is still intact (i.e., for cases of reactivity excursion and inadequate flow without scram), the assumptions of void fraction in the explosion

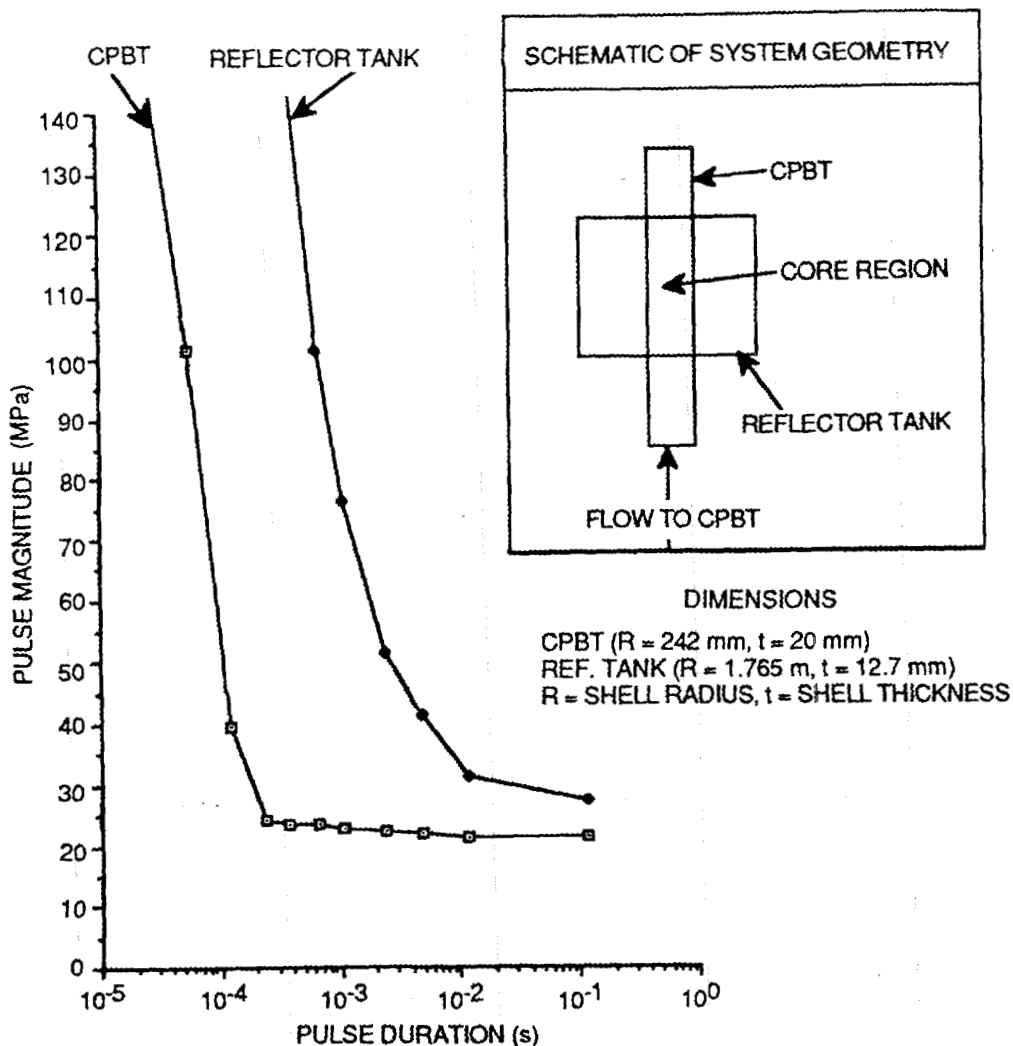


Fig. 17. ANS failure envelopes for CPBT and reflector tank.

zone need to be made carefully because for flows through narrow channels, a low-flow quality can sometimes lead to large void fractions. Hence, the cases of void fractions of ~90% are considered as part of a parametric study for failure analyses of two cases for which the core geometry is intact before the explosion. The precise value will obviously depend on the operating conditions during the transient. However, it should be kept in mind that a large void fraction in these instances does not necessarily imply the absence of a significant liquid flow rate with which the molten metal needs to interact to produce a steam explosion.

Based on the results given in Figs. 13 and 14, the case of reactivity excursion without scram (described in Appendixes A and B) can be expected to give rise to pressure-pulse magnitudes of ~87.5 MPa. This

assumes a coolant-to-fuel mass ratio of 1.0 and coolant-void fraction of ~30% in the explosion zone. For coolant-void fractions of 15 and 90%, the pulse magnitudes obtained can be ~75 and 24 MPa, respectively, assuming a coolant-to-fuel mass ratio of 1.0. Under the assumption of a coolant-to-fuel mass ratio of 0.5, the corresponding values of pulse magnitudes for 15, 30, and 90% void fractions can be found to be 120, 125, and 30 MPa, respectively. For all these pulse magnitude levels, CPBT can definitely be expected to fail. Failure of the reflector tank is not easy to gage because of the low pulse magnitude levels associated with high (i.e., 90%) void fractions and the absence of pulse duration times. However, it may be conservatively assumed that the reflector tank integrity will be severely challenged, with failure to be expected for cases without excessive void fraction (i.e., ~90%).

The case of inadequate cooling without scram is expected to give rise to peak pressure-pulse magnitude levels of ~220, 192, and 37 MPa for coolant void fractions of 15, 30, and 90%, respectively, assuming a coolant-to-fuel mass ratio of 0.5. Pulse magnitudes of 121, 123, and 28 MPa are expected for void fractions of 15, 30, and 90%, respectively, assuming a coolant-to-fuel mass ratio of 1.0. Once again, despite the large range of predicted pressure-pulse magnitude levels, it is clear that CPBT can be expected to fail. This transient is more likely than the earlier case (i.e., reactivity excursion with scram) to challenge the integrity of the reflector vessel because of the higher fuel temperature and thus peak pressure levels. Once again, failure of the reflector tank may be expected when the coolant void fraction in the explosion zone is not excessive (i.e., ~90%).

For the case of inadequate cooling on decay heat, the scenario that would most suitably apply to events in CPBT are those that involve a loss of coolant in the core region resulting from boil-off. The core can then be expected to melt and slump, as in conventional LWR scenarios (Fig. 1), into a pool of water. From Figs. 13 and 14, the following pressure-pulse magnitudes are predicted for coolant-void fractions of 15 and 30%, respectively: (1) pulse magnitudes of 60 and 72 MPa, assuming a coolant-to-fuel mass ratio of 0.5, and (2) pulse magnitudes of 30 and 46.5 MPa, assuming a coolant-to-fuel mass ratio of 1.0. Once again, CPBT can be expected to fail. However, the reflector tank may be expected to remain intact with a reasonable safety margin, assuming a pulse duration of ~1 ms or less, as observed experimentally²⁰ under similar conditions.

An interesting feature in Fig. 17 is that the failure pulse magnitude of 22 MPa for CPBT (i.e., for pulse durations of >0.2 ms) is close to the static limit for failure, which is ~20 MPa. Assuming that other possible structural materials give rise to a similar profile, they can also be analyzed for integrity in the event of steam explosions. It is recognized that Al-6061 is the material of choice because of other design considerations. However, stainless steel and Zircaloy-2 were considered to provide a perspective and a basis for comparison. Comparable dynamic limits that were generated for Zircaloy and stainless steel are shown in Table 9. As noted in the table, stainless steel, if

Table 9. Limiting pressure-pulse magnitudes for CPBT and reflector tank fabricated with various materials

(Pulse duration ~1 ms)

Material ^a	Yield stress (MPa)	Limiting dynamic pressure (MPa) ^{b, c}	
		CPBT	Reflector tank
Al-6061	219	22	75
Zircalloy-2	288	29	99
Stainless steel	431	43	148

^aGeometrical configuration for all three cases is assumed to be identical.

^bLimiting dynamic pressures for CPBT and reflector tank fabricated with Al-6061 were taken from Fig. 17.

^cLimiting dynamic pressures for CPBT and reflector tank fabricated with Zircalloy-2 or stainless steel =

$$\text{Limiting pressure with Al-6061} \times \frac{\text{yield stress (Zr-2 or steel)}}{\text{yield stress (Al-6061)}} .$$

used for CPBT and reflector tank construction, may provide up to twice the capability of withstanding pressure pulses compared with Al-6061.

The second and more important phase of the transient, from the standpoint of safety, is also more difficult to analyze. As mentioned previously, the actual dynamics of destructive processes and possible missile generation would require knowledge of geometry and operating conditions as well as the methodology outlined in Chap. 3. In the absence of these tools and information, a qualitative analysis was performed based on the parametric evaluations shown in Figs. 15 and 16.

For the cases of reactivity excursion and inadequate cooling without scram, both of which are postulated to occur with RCS full of water, no mechanism is now envisioned for directly producing potentially destructive missiles or slugs. In these instances, the second phase of the steam-explosion event would cause rapid loop pressurization. Recall, however, that the first phase of the steam-explosion event may have already failed the CPBT and the reflector tank. However, for simplicity and to obtain order-of-magnitude estimates of RCS pressurization levels, this phase is treated separately (i.e., assuming that CPBT is

still intact). Based on the mechanical energy available for coolant compression in RCS, both from thermodynamic and best-estimate stand-points, estimates were obtained for loop pressurization and are given in Table 10. Note that these pressurization levels were estimated assuming that the entire RCS coolant pressurizes simultaneously. Even so, the resulting pressure levels amount to several times the CPBT design value of ~6 MPa. The RCS can then be expected to rupture at its weakest section. Depending on the location of the rupture, the resulting slug energetics generation and propagation will affect confinement integrity differently. This issue, which would require further investigation, has no parallel in the extensive work performed for commercial LWR steam-explosion analysis.

For the case of inadequate cooling on decay heat where molten fuel drops into a pool of water located below a void space, energetic slug generation becomes a direct possibility for in-vessel and ex-vessel steam explosions. Once again, the velocity of a slug mixture would depend upon several factors, one of them being the amount of available water to which mechanical work can be imparted. Based on available mechanical energy, slug velocities were estimated for a variety of expected masses using Fig. 15. These values are tabulated in Table 11.

Table 10. Estimates of ANS RCS pressurization levels from expansion phase of steam explosions

Scenario	RCS loop pressurization ^a levels (MPa)		
	Energy of compression assumptions ^b		
	Thermodynamically based		Experimentally based
	Upper bound ^c (mechanical)	Best estimate (mechanical)	Best estimate (mechanical)
Reactivity excursion without scram	50	35.3	20.7
Inadequate cooling without scram	61.5	43.4	24.3

^aCompression volume = 114 m³ (i.e., the entire RCS volume).

^bEnergy of compression values taken from Table 7.

^cMechanical energy of compression is taken as twice the best-estimate thermodynamic mechanical energy (Appendix A).

Table 11. Estimates of ANS slug energetics from expansion phase of steam explosions

Slug mass (kg)	Slug velocity (m/s)		
	Mechanical energy availability assumptions ^a		
	Thermodynamically based		Experimentally based
	Upper bound (mechanical)	Best estimate (mechanical)	Best estimate (mechanical)
35	1398	988	607
100	827	585	359
200	585	413	254
2000	185	131	80.3

^aAvailable mechanical energy values taken from Table 7 for the scenario in which molten fuel mixture (generated because of inadequate cooling on decay heat) drops into a pool of coolant and then undergoes a steam explosion.

As noted in the table, slugs can be generated with velocities close to sonic levels (i.e., speed of sound in water under standard temperature and pressure conditions). The propagation of these slugs and the possible generation of missiles with the potential of breaching the containment is a subject that needs careful investigation but is beyond the scope of this report.

It should be recognized, however, that the above evaluations of slug velocities and loop pressurization are conservative estimates. The experimentally based best-estimate value for the conversion ratio of 10% may not be readily achievable. Again, slug velocities evaluated from Eq. (4.3) should be considered as being the highest achievable values for a given amount of mechanical energy, because multidimensional aspects such as slug dispersion and breakup have not been included in its formulation. Thus, in light of the many assumptions that have been made, the results presented herein should be considered preliminary, to be used for scoping purposes only. The results do indicate that, in the absence of designed preventive and mitigative features, a potential exists for the generation of damaging pressure pulses, loop overpressurization-induced failure, and the evolution of energetic slugs.

6. SUMMARY AND CONCLUSIONS

This report has focused on the subject of steam explosions and their applicability to nuclear reactors, with specific emphasis on ANS. An overview was given of previous experiments and analytical work conducted to provide an understanding of steam-explosion phenomena. The report has also provided a preliminary steam-explosion analysis for ANS. Peak pressure-pulse magnitudes and slug energetics were evaluated and then used to conduct a failure analysis.

Based on the work performed as part of this preliminary study, several major conclusions can be derived. These are enumerated below.

6.1 PROPENSITY FOR ENERGETIC STEAM-EXPLOSION OCCURRENCE IN ANS

It was found that the current ANS design satisfies well-established criteria that predict the possibility of steam explosions in the event of a core melt. These same criteria were also met in previous plate-type, aluminum-clad research reactors. In the examples considered here (i.e., SPERT-1, BORAX-1, and the SL-1 incident), severe damage occurred (during destructive prompt critical nuclear reactivity excursions) not only to the core, but also to the reactor building, thereby showing the nature of the loading mechanisms.

An extensive review of out-of-reactor experiments showed that except under tightly controlled conditions, high-temperature molten aluminum and its oxide can explode spontaneously when brought into intimate contact with water on a wettable surface, without the need for an external trigger. Such an intimate contact or mixing can occur when the melt drops onto a solid surface. Based on recent experiments and analyses, it was noted,²² however, that only certain aluminum alloy melts, with and without superheat, undergo spontaneous explosions (without solid-melt contact) when poured in water. Fortunately, Al-6061 is not one of those alloys. However, upon contact with a wettable (e.g., concrete) solid surface, spontaneous explosions can occur. No information now exists for the propensity of molten U_3Si_2/Al mixtures to undergo spontaneous explosions. Such fundamental information would be very useful to have and could be obtained via small-scale experiments. These experiments would evaluate trigger energy levels necessary for explosions to occur. In the absence of such information, a steam explosion should be expected to occur in ANS during accidents when molten fuel is brought into contact with water. The actual damage-producing pressure pulses and energetic slug loadings will depend on specific operating conditions.

6.2 DAMAGE POTENTIAL FROM STEAM EXPLOSIONS IN ANS

A preliminary steam-explosion analysis for ANS was conducted. Pressure-pulse magnitudes, RCS loop pressurization levels, and slug energetics were evaluated. The model used for the evaluation of pressure pulses was benchmarked against previous calculations, an aluminum-water steam-explosion experiment, and steam explosion data from test reactor experiences. Good agreement was obtained. Parametric calculations were conducted over a wide range of expected fuel temperatures, coolant-to-fuel mass ratios, and coolant-void fractions. Sensitivity to key parameters was noted. Thereafter, preliminary scoping evaluations were performed for three ANS accident scenarios: (1) reactivity excursion without scram, (2) inadequate primary coolant flow without scram, and (3) inadequate cooling on decay heat. A failure analysis for the CPBT and reflector tank from initial pressure pulses immediately following a steam explosion was also conducted. The analysis indicated the following:

1. For pressure-pulse durations of ~1 ms, the CPBT and reflector tanks can withstand pulse magnitudes of up to 22 and 75 MPa, respectively. Based on predicted pressure-pulse magnitudes over a range of coolant-void fractions and coolant-to-fuel mass ratios in the explosion zone, it was estimated that CPBT failure can be expected for all three cases considered. The integrity of the reflector tank would be severely challenged, and failure may occur for the cases of reactivity excursion and inadequate cooling without scram if the coolant-void fraction in the explosion zone is not excessive (i.e., ~90%). However, it was estimated that for the case of inadequate cooling on decay heat, the reflector tank may be expected to remain intact with a reasonable safety margin.

Scoping estimates were also derived by assuming the same geometry for the CPBT and reflector tanks (but fabricated with Zircaloy-2 or stainless steel material). The corresponding limits of pressure-pulse magnitude tolerance without failure are greater than those for Al-6061 by 31 and 100% for Zircaloy-2 and stainless steel, respectively. Because of uncertainties in the various key parameters (namely, coolant void fraction and pulse duration), it is difficult to judge whether the use of these higher strength materials would have any effect on whether the CPBT and reflector tanks would fail or not. However, this preliminary analysis does demonstrate that these materials would provide for significantly increased margins to failure than Al-6061.

2. The later phase of the steam explosion may lead to significant RCS loop pressurization to many times the ANS design pressure capability for a "solid" system. For a conventional LWR-type scenario, during which molten fuel dislocates and then interacts with a pool of water with a void volume above it, energetic slugs may be generated traveling at speeds comparable to sonic levels. In both instances, the actual dynamics of the destructive processes and missile generation would require knowledge of geometry and operating conditions, as well as methodology outlined in Chap. 3. However, engineering judgment indicates that significant damage potential exists and should be guarded against by design whenever possible.

6.3 EXTENT OF ANALYSIS FOR ANS

Note that steam explosions in commercial reactors are analyzed as occurring when molten corium dislocates and then interacts with a pool of water in the lower plenum. For the ANS design, analysis will require, in addition, considering the case of rapid reactivity insertion with an intact core geometry. The situation would parallel SPERT and other destructive events.

State-of-the-art analyses typically involve the use of wave codes in conjunction with finite-element (or other) structural calculations. Ex-vessel steam-explosion event possibilities and resulting containment damage potentials are also considered to judge their relevance to safety and design.

6.4 MODELING OF DESTRUCTIVE LOADINGS FROM STEAM EXPLOSIONS VS CHEMICAL DETONATIONS

It was demonstrated that steam explosions manifest themselves quite differently from chemical detonations. Destructive loadings from steam explosions can be separated into two time phases. In the early (≤ 5 -ms) time phase, immediately following a steam explosion, the loading is primarily caused by pressure pulses, which are ~ 100 MPa. These are in sharp contrast to pressures generated from explosives, which are $\sim 10^5$ MPa. Indeed, the pressure-pulse magnitudes calculated in this report for various accident scenarios were several orders of magnitude smaller than equivalent values obtained through the correlation of available energies with chemical detonation-related pressure-pulse levels. This finding clearly attests to the inappropriateness of modeling steam explosions as chemical detonations. It can also lead to needless overconservatism and result in misleading design and safety conclusions because the true damage potential of steam explosions arises in the later time phase when high-pressure vapor expands, causing RCS loop overpressurization failure and possibly creating a highly energetic slug. It is this slug that, on impact with the pressure boundary, may cause rupture and generate missiles that might then breach the outer containment. The thermal-to-mechanical energy conversion process is also quite different from steam explosions and chemical detonations. This aspect is evidenced from the experiment described in Ref. 39, where the measured conversion ratio of detonation-driven explosions was found to be significantly different from that seen for steam explosions.

7. RECOMMENDATIONS

Based on the analysis conducted for the ANS core region, it was concluded that a CPBT designed with aluminum-6061 would be incapable of withstanding high-pressure pulses generated immediately following a steam explosion. The situation in the later phase of a steam-explosion transient, based on best-estimate and conservative calculations, may lead to extensive overpressurization and failure of the RCS loop and may also generate highly energetic slugs with velocities in the sonic range. Destruction of CPBT and containment failure caused by missile penetration may occur during this phase.

To develop a robust ANS design with acceptably low risks to public health as well as plant investment, an integrated treatment of steam-explosion issues will be necessary. The following recommendations and ANS Project policy statements are presented in the interest of furthering this goal.

1. The paramount importance that is now given to the design of ANS safety and control systems will be continued. The analysis and scoping calculations given in previous sections clearly demonstrate that reactivity excursions without a rapid reactor scram that cause high-temperature molten aluminum to come in contact with water can be extremely destructive. Hence, great care will be taken during the design phase of the ANS project to preclude the possibility of such reactivity excursions. It may be necessary to perform additional analyses of the type discussed in Chap. 5 to determine acceptable levels or safety margins for positive reactivity insertion without scram.

2. The simulation of anticipated transient without scram events needs to be improved to quantify conditions better at the time of average channel burnout (if applicable). The methods used in Appendixes A and B to estimate peak fuel temperatures following the limiting design-basis ATWS event did not have sufficient thermal-hydraulic sophistication to calculate the reactivity effects of boiling phenomena that would precede burnout.

3. The ANS probabilistic risk assessment (PRA) effort should provide for a detailed examination of events leading to fuel melting and the contribution of steam explosions to the containment-failure event tree. It is anticipated that analyses of the type described in this report will need to be undertaken to evaluate the probability of containment failure following a steam explosion in ANS. This analysis would essentially entail the approach outlined in Chap. 3. The analytical tools described in this report would be used parametrically to develop a robust reactor design and highlight design weakness at an early stage.

4. If the ANS PRA indicates a significant probability of reactivity-induced transient and/or core-melt accidents, the ANS Project will establish (or use) a state-of-the-art capability for analyzing steam-explosion events. As mentioned previously, the various phenomena in a steam-explosion event are not well understood. Research is still being conducted worldwide. Hence, an engineering approach toward evaluation of the propagation and expansion phases is suggested. Such an approach was taken for NRC-sponsored studies as applied to commercial reactors, entailing the implementation of a wave code package (see Chap. 3) that is available from SNL, along with a finite-element structural simulation capability for failure analysis. Such a structural analysis capability already exists in-house at Oak Ridge National Laboratory (ORNL) and at other laboratories. The overall analytical package would thus provide an interactive analysis framework for application during the ANS design evolution.

5. As noted in previous sections, the propensity of molten aluminum mixtures for undergoing spontaneous explosions is highly dependent on mixture composition and available triggers (if any). No information now exists for molten Al-6061/U₃Si₂ mixture interactions with water. It would thus be highly desirable to obtain such fundamental (experimentally derived) information to evaluate trigger-energy levels required for FCI occurrence. If the observed trigger-energy levels are found to be physically unattainable, then it may be possible to consider FCI occurrence in ANS to be a low-probability event.

Initial steps have already been taken to implement some of those recommendations. Available literature on the subject has been extensively reviewed and assimilated. Key individuals working in this field have been identified (Appendix C). The basic rules of thumb for steam-explosion-generated loading evaluations have already been developed, as discussed in this report. Additionally, the overall framework for implementing an effective failure analysis has also been extensively studied. Therefore, it would be possible for ORNL to establish an efficient, state-of-the-art capability to analyze steam-explosion issues related to the ANS design.

These recommendations would allow for a responsive, synergistic in-house approach between design and safety functions for resolving this important issue and also for minimizing risks to the environment and plant investment.

REFERENCES

1. *Reactor Safety Study*, WASH-1400, NUREG/75-0114, 1975.
2. J. R. Dietrich, *Experimental Investigation of the Self-Limitation of Power During Reactivity Transients in a Subcooled, Water-Moderated Reactor. BORAX-I Experiments*, ANL-5323, Argonne Natl. Lab., March 1957.
3. R. W. Miller et al., *Report of SPERT-I Destructive Test Program on an Aluminum, Plate-Type, Water-Moderated Reactor*, IDO-16883, June 1964.
4. *Final Report of SL-1 Recovery Operation, May 1961-July 1962*, IDO-19311, July 1962.
5. J. F. Junz (ed.), *Additional Analysis of the SL-1 Excursion*, IDO-19313, November 1962.
6. S. G. Bankoff et al., *Steam Explosions - Their Relationship to LWR Assessments*, NUREG/CP-0027, Vol. 2, August 1982.
7. S. G. Bankoff, "Vapor Explosions: A Critical Review," *Proc. 6th Intl. Heat Transfer Conference*, Vol. 6, pp. 355-60, 1978.
8. R. M. Harrington, "Notes on ANS Core Disruption Thermodynamics," *Internal Correspondence*, Oak Ridge Natl. Lab., May 1988.
9. M. Corradini, "Analysis and Modelling of Large-Scale Steam Explosion Experiments," *Nucl. Sci. Eng.* 82, 429-47 (1982).
10. M. Corradini, *Analysis and Modelling of Steam Explosion Experiments*, NUREG/CR-2072, April 1981.
11. L. Nelson and L. D. Buxton, *Steam Explosion Triggering Phenomena: Stainless Steel and Corium-E Simulants Studied with a Floodable Arc Melting Apparatus*, NUREG/CR-1022, May 1978.
12. L. Nelson et al., *Steam Explosion Triggering Phenomena; Part 2: Corium-A and Corium-E Simulants and Oxides of Iron and Cobalt Studied with a Floodable Arc Melting Apparatus*, NUREG/CR-0633, May 1980.
13. L. Buxton and W. Benedick, *Steam Explosion Efficiency Studies; Part 1*, NUREG/CR-0947, October 1980.
14. T. G. Theofanous et al., *Nucl. Sci. Eng.*, 97, 259-316 (1987).
15. G. Long, "Explosions of Molten Aluminum in Water - Causes and Prevention," *Met. Prog.* 71 (May 1957).

16. P. D. Hess and K. J. Brondyke, "Causes of Molten Aluminum-Water Explosions and Their Prevention," *Met. Prog.* 45 (April 1969).
17. J. A. Dunbar, "Guidelines for Handling Molten Aluminum in Casting Operations," *Light Metals 1980*, ed. C. J. McMinn, Metallurgical Society of AIME, Warrendale, Penn., 1980, pp. 887-98.
18. P. D. Hess et al., "Molten Aluminum/Water Explosions," *Light Metals 1980*, ed. C. J. McMinn, Metallurgical Society of AIME, Warrendale, Penn., 1980, pp. 837-57.
19. A. W. Lemmon, Jr., "Explosions of Molten Aluminum and Water," *Light Metals 1980*, ed. C. J. McMinn, Metallurgical Society of AIME, Warrendale, Penn., 1980, pp. 817-36.
20. C. J. Fry et al., *CSNI Joint Interpretation Exercise on Fuel-Coolant Interactions. Results from Selected Experiments Performed in the Thermir Facility at AEE Winfrith, AEEW-M-1778*, UKAEA Atomic Energy Establishment, Winfrith, United Kingdom, May 1980.
21. L. Nelson et al., "Initiation of Explosive Molten Aluminum-Water Interactions at Wet or Underwater Surfaces," *1988 ASME/AICHE National Heat Transfer Conference*, Houston, July 1988.
22. Personal communication to R. P. Taleyarkhan, Oak Ridge Natl. Lab., from Lloyd Nelson, Sandia National Laboratories.
23. Personal communication to R. P. Taleyarkhan, Oak Ridge Natl. Lab., from M. Lee Hyder, Savannah River Laboratory.
24. M. Corradini, "Molten Fuel/Coolant Interactions: Recent Analysis of Experiments," *Nucl. Sci. Eng.* 86, 372-87 (1984).
25. M. Berman, *Light Water Reactor Safety Research Program Semi-Annual Report, October 1981-March 1982*, NUREG/CR-2841, October 1984.
26. H. Fauske, "Some Aspects of Liquid-Liquid Heat Transfer and Explosive Boiling," *Proceedings of the Fast Reactor Safety Meeting, Beverly Hills, California, CONF-740401*, April 1974.
27. M. Corradini and D. Swenson, *Probability of Containment Failure due to Steam Explosions Following a Postulated Core Meltdown in an LWR*, NUREG/CR-2214, June 1981.
28. *Reactor Safety Research Semi-Annual Report, July-December 1986*, NUREG/CR-4805, VOL. 36, (SAND86-2752), Sandia National Laboratories.
29. S. Thompson, *CSQ-II, An Eulerian Finite Difference Program for Two-Dimensional Material Response*, SAND77-1339, Sandia National Laboratories, February 1979.

30. R. Lawrence and D. Mason, *WONDY-IV, A Computer Program for One-Dimensional Wave Propagation with Rezoning*, SC-RR-710284, 1975.
31. L. Nelson and L. Buxton, *Steam Explosion Triggering Phenomena: Stainless Steel and Corium-E Simulants Studied with a Floodable Arc-Melting Apparatus*, NUREG/CR-0122, May 1978.
32. A. Ghosh, "A Criterion for Ductile Fracture in Sheets Under Biaxial Loading," *Metal. Trans.*, 7A (April 1976).
33. S. Key et al., *HONDO-II, A Finite Element Computer Program for the Large Deformation Dynamic Response of Axisymmetric Solids*, SAND78-0422, Sandia National Laboratories, October 1978.
34. C. Young, *Empirical Equation for Projectile Penetration in Layered Earth Material and Concrete Penetration*, SC-DR-72-0523, December 1972.
35. D. Berriaud, *French Program for the Study of the Effects of Projectile Impacts on Reinforced Concrete Walls*, 4th SMIRT Conference, CEA-EDF, San Francisco, 1976.
36. C. Berraud, "Rigid Missile Penetration in Concrete Reinforced Wall," *POST-4th SMIRT SEMINAR, Prob. and Extreme Load Design of Nuclear Power Plants*, San Francisco, 1976.
37. R. Gwaltney, "Steam Explosion in the Core Pressure Boundary Tube," *Internal Correspondence*, Oak Ridge Natl. Lab., July 1988.
38. R. Gwaltney and C. Luttrell, *Development of a Failure Envelope for Triangular Pressure Impulse Loads*, ORNL/ANS/INT-5/V8, Martin Marietta Energy Systems, Inc., Oak Ridge Natl. Lab., November 1988.

APPENDIX A

NOTES ON ANS CORE-DISRUPTION THERMODYNAMICS

R. M. Harrington

These preliminary notes provide estimates of the approximate quantities of energy required to heat, melt, and vaporize a representative ANS core.

A.1 ALUMINUM AND U_3Si_2 PROPERTIES

The following properties of aluminum and U_3Si_2 as were taken from the report ANL/RETR-11:

aluminum density = 2.72 kg/L,

U_3Si_2 density = 12.2 kg/L,

aluminum specific heat (J/kgK) = $892 + 0.46 T$, where T is °C,

U_3Si_2 specific heat (J/kgK) = $199 + 0.104 T$, where T is °C, and

aluminum (6061) melting range = 582°C solidus, 649°C liquidus.

For the calculations in this appendix, aluminum melting is represented as a point phenomenon occurring at 600°C:

aluminum heat of fusion = 3.96 E-4 MJ/g,

aluminum heat of vaporization = 1.05 E-2 MJ/g, and

aluminum boiling point (atmosphere pressure) = 2327°C.

A.2 ENERGY REQUIREMENTS

The ANS preconceptual core has an active fuel volume of ~67.4 L, of which half is coolant and half is fuel. Of the 33.7 L of fuel, roughly half is the U_3Si_2 /aluminum meat, and half is the aluminum clad. The meat is ~10% by volume U_3Si_2 and 90% aluminum powder (voids neglected). Therefore, the masses are as follows:

mass aluminum = $2.72 \text{ kg/L} \times (16.8 \text{ L clad} + 0.90 \times 16.8 \text{ L meat}) =$

86.8 kg, and

mass U_3Si_2 = $12.2 \text{ kg/L} \times (0.10 \times 16.8 \text{ L meat}) = 20.5 \text{ kg}.$

Phase 1: Heating from Normal Temperature to the Melting Point

Normal temperature is taken to be 300°C, which is below the 380°C limit on fuel centerline temperature for satisfactory normal fuel performance:

$$\begin{aligned} dE &= (M_{Al} \times C_{p,Al} + M_{U_3Si_2} \times C_{p,U_3Si_2}) \times (600^\circ\text{C} - 300^\circ\text{C}) \\ &= (86.8 \text{ kg Al} \times 1099 \text{ J/kgK} + 20.5 \text{ kg } U_3Si_2 \times 245 \text{ J/kgK}) \\ &\quad \times 300 \text{ K} = 30.1 \text{ MJ.} \end{aligned}$$

Phase 2: Melting

This calculation determines the energy required to melt the 86.8 kg of aluminum with conservative consideration of the possible energy input from the chemical reaction between U_3Si_2 and aluminum powder (400 J/g of U_3Si_2):

$$\begin{aligned} dE \text{ (required)} &= 86.8 \text{ kg Al} \times 3.96 \text{ E-4 MJ/g} = 34.4 \text{ MJ} , \\ dE \text{ (from reaction)} &= 400 \text{ J/g} \times 20.5 \text{ kg} = 8.2 \text{ MJ} , \\ dE \text{ (required, net)} &= 34.4 \text{ MJ} - 12.2 \text{ MJ} = 26.2 \text{ MJ.} \end{aligned}$$

Phase 3: Heating from the Melting Point to the Boiling Point

This calculation determines the energy required to heat the molten aluminum from its melting point halfway to its boiling point.

$$\begin{aligned} de &= (1463 - 600) \times (86.8 \text{ kg Al} \times 1366 \text{ J/kgK}) \\ &\quad + 20.5 \text{ kg} \times 306 \text{ J/kgK} = 108 \text{ MJ.} \end{aligned}$$

Phase 4: Heating from the Melting Point to the Boiling Point

This calculation determines the energy required to heat the molten aluminum from its melting point to its boiling point.

$$dE = (2327 - 600) \times (47.6 \times 1565 + 30.5 \times 351) = 247 \text{ MJ.}$$

Phase 5: Boiling

This calculation determines the energy required to boil off the molten aluminum at its boiling point.

$$dE = 86.8 \text{ kg Al} \times 1.05 \text{ E-2 MJ/g} = 911 \text{ MJ.}$$

A.3 CORE DISRUPTION TIMES

The time required for core disruption depends on the energy available. In general, the energy available for core disruption is equal to the energy production rate minus the cooling rate. The worst case would be some sort of a reactivity excursion without scram that increases power to >100% while simultaneously causing DNB and burnout in the core. The most benign case would be overheating on decay heat.

Event	Approximate bounding heating rate (% of full power)	Disruption time (ms)
Reactivity excursion without scram (see Appendix B)	275	59
Loss of coolant flow from full power	100	290
Inadequate cooling after shutdown	1 to 6	320

Table A.1 summarizes the times required to reach the various stages of core disruption for different net core heating input rates.

Table A.1. Hypothetical ANS core-disruption times

Heating rate (MW)	Time to reach indicated condition/ temperature from 300°C (initial temperature = 300°C)				
	600°C (solid) (30 MJ)	600°C (molten) (56 MJ)	1463°C (molten) (164 MJ)	2327°C (molten) (303 MJ)	2327°C (vapor) (1214 MJ)
3500	8.6 ms	16 ms	47 ms	87 ms	347 ms
350	86 ms	160 ms	470 ms	866 ms	3.46 s
175	171 ms	320 ms	937 ms	1.73 s	6.94 s
120	250 ms	467 ms	1.36 s	2.52 s	10.1 s
70	428 ms	800 ms	2.34 s	4.33 s	17.3 s
35	857 ms	1.6 s	4.69 s	8.65 s	34.7 s
17.5	1.71 s	3.2 s	9.37 s	17.3 s	69.4 s
7	4.3 s	8 s	23.4 s	43.3 s	173 s
3.5	8.6 s	16 s	6.48 s	86.6 s	347 s

A.4 LIMITS ON POWER EXCURSIONS AND HEATUPS

If an appropriate scram has not occurred, the core will continue to increase in temperature until the fuel is redistributed from the core. This event could happen in several ways: (1) the molten fuel drops out of the core under the influence of gravity or (2) the molten fuel is expelled from the core by hydraulic forces (with the pumps still running). The time scale for each of these mechanisms is estimated as follows:

$$\text{Gravity: } t = \sqrt{2 s/g} = \sqrt{2 \times 0.5 \text{ m}/10 \text{ m/s}^2} = 0.32 \text{ s} .$$

Flow at nominal:

flow velocity, between the plates = 27 m/s;

flow velocity, upstream core inlet = 13.5 m/s;

relative velocity required to sweep debris up and out of the core = 5 m/s (see Appendix B);

net sweep velocity = 13.5 - 5 = 8.5 m/s; and

$$t = s/v = 0.5 \text{ m}/(8.5 \text{ m/s}) = 0.059 \text{ s} .$$

Flow at 1/2 nominal:

flow velocity (between the plates) for inadequate cooling (50% flow) with power still at 100% = 13.5 m/s;

flow velocity, just upstream of core inlet (50% flow) = 6.75 m/s;

relative velocity necessary to sweep debris up/out of core = 5 m/s;

net sweep velocity = (6.75 - 5) m/s = 1.75 m/s; and

$$t = s/v = 0.5 \text{ m}/(1.75 \text{ m/s}) = 0.295 \text{ s} .$$

Now consider how these processes would limit different types of severe accident heatups.

A.4.1 Reactivity Excursion Without Scram

For this type of core destruction event to occur, it is necessary to postulate not only that a super-prompt-critical amount of reactivity is suddenly inserted, but also that the reactor protection system fails to initiate the rapid insertion of the control rods. The reader

is referred to Appendix B for the reactivity excursion analysis. The results are as follows:

bounding debris energy = 121 MJ, and

maximum temperature of molten fuel = 1054°C.

A.4.2 Inadequate Cooling Without Scram

For this type of power mismatch to occur, it must be assumed that the rapid insertion of control rods (scram) has, for some reason, failed to take place and that the control system has failed to insert control rods to maintain the desired balance between power generation and available cooling.

Assuming power constant at 100% and continued, but inadequate, primary coolant flow (e.g., 100% power with only 50% flow), the flow would take ~290 ms to sweep out the fuel after it becomes molten (as calculated previously). Table A.1 shows that it takes ~160 ms for the core to become fully molten at the melting point. During the 290 ms that would elapse while the flow is sweeping out the molten fuel, its temperature would continue to increase, reaching 1411°C if we assume that the power remains constant at full power. The fuel would be dispersed after being swept from the core and would be subcritical. Further heating might continue in a debris bed but under different conditions and under lower decay-heat power conditions. An upper limit on the energy of debris (relative to 300°C, according to Sect. A.2) in this heatup event would be 166 MJ. This is considered a bounding estimate because inherent negative feedback mechanisms that would tend to depress power during a primary coolant flow coastdown have been ignored. (This simplistic hand calculation ignores both temperature and rod feedback, both of which would be negative.)

A.4.3 Inadequate Cooling after Scram (Decay Heat Power)

Referring again to Table A.1, we see that adiabatic heating on decay heat levels (17.5 MW and below) would take 3.2 s (at 17.5 MW) or longer (e.g., 16 s at 3 MW) to melt the core totally. Because the gravity drop time is only 0.32 s, it appears that the hotter portions of the fuel would begin dribbling out before the whole core is totally molten. However, it would be difficult to predict how much of the core would drop or flow out before the other parts do. For example, portions of the fuel that have the highest power density would achieve the liquidus point and have more than enough time to fall out of the core before those of average power density. One can certainly conclude, however, that the whole core might become molten but would not, on the average, have time to heat to above the liquidus point before being removed from the core region. Therefore, a reasonable upper limit on core debris energy for this type of meltdown would be 64.5 MJ, but it seems very unlikely that a coherent molten mass would be dropped into the subcooled water below the core.

A.5 STEAM EXPLOSION VS RAPID STEAM GENERATION

When the molten core leaves the core region, it enters a region of subcooled water and will be rapidly cooled, generating steam in the process. The steam will be rapidly condensed because the water is subcooled. Whether the debris/water interaction is classified as a rapid steam generation or as a steam explosion depends on whether the debris breaks up into small enough particles when it hits the subcooled water region. If the particles are small (e.g., 1 mm), most of the energy can be transferred from debris to water in less time than it takes for the resulting shock wave to communicate with the rest of the coolant system. This is a steam explosion. If the particles are ten times larger (e.g., 10 mm), the increased pressure has time to be felt throughout the entire coolant system, and this is not a steam explosion. These points are illustrated arithmetically as follows:

$$\text{Biot modulus of particles} = hRO/k ,$$

where

- h = heat transfer coefficient between the surface of the sphere and the coolant,
- RO = the radius of the sphere,
- k = the thermal conductivity of the sphere.

Therefore, $Bi = 2.1$ for a 1-mm radius sphere of aluminum, and $Bi = 21$ for a 10-mm radius sphere.

To estimate the transient response of the debris "spheres," we will rely on the family of curves of Q/Q_0 vs Bi in Kreith¹ (Fig. 4.13) with dimensionless time (time \times thermal diffusivity/ RO^2), defining the different response curves. The time required to transfer 50% of the stored heat (i.e., when $Q/Q_0 = 0.5$) is calculated as follows:

For $Bi = 2$, ($RO = 1$ mm),

$Q/Q_0 = 0.5$ when dimensionless time = 0.25, or when actual time = 2.9 ms.

For $Bi = 20$, ($RO = 10$ mm),

$Q/Q_0 = 0.5$ when dimensionless time = 0.09, or when actual time = 105 ms.

If CPBT is ~10 m long, it will take ~5 m/(1500 m/s) or 3.33 ms for a shock wave to exit from CPBT into the remainder of the coolant system. Therefore, a significant portion of the energy from the 1-mm particles could be transferred to steam before the pressure wave could get out of CPBT. These criteria fulfill the definition of a steam explosion.

On the other hand, for the 10-mm radius particles, the shock wave could travel to every part of the RCS in the 105 ms it takes to transfer half of the stored thermal energy to the water. Such an event would not represent a steam explosion. Moreover, it would seem likely that a significant portion of the steam generated over this relatively long period would be condensed because of contact with the subcooled water.

Experiments conducted at the Thermir facility at Winfrith have demonstrated that it is possible to get steam explosions with molten aluminum and tin. Of course, small explosive charges were needed to fragment the molten metal sufficiently -- just pouring the 850°C molten charge into subcooled water was not adequate to initiate the steam explosion. Those experiments demonstrated that steam explosion is possible without showing us how likely it is. The SPERT-I destructive test at Idaho showed that an intentional power excursion (time to increase power level by a factor of 2.72) of 3.2 ms did cause a steam explosion. To get the SPERT-I UAL_x core on a 3.2-ms period, the transient rod was intentionally ejected, thus inserting a reactivity of \$3.55 (i.e., 3.55 times the minimum amount needed to bring the reactor to "prompt" critical). The ANS research reactor will be designed to make such an occurrence highly unlikely, if not impossible.

A.6 ENERGY AVAILABLE FOR STEAM EXPLOSION IN CPBT

This section makes a conservative estimate of the amount of energy the CPBT would have to absorb to withstand the initial pressure pulse of a steam explosion. To avoid being ultraconservative, several factors will be considered that would place limits on the energy available for damaging CPBT:

1. Not all the mass of the core would reach the 1 mm or smaller particle size needed for a steam explosion.
2. Even for 1-mm radius particles, not all of the thermal energy would be transferred quickly enough to participate in the steam explosion. We will, as calculated in Sect. 3, assume that one-half of the thermal energy can be transferred quickly enough such that only CPBT would have to withstand its effects.
3. In even a severe core damage accident, not all of the core would become molten at the same time. Accident experience suggests that 50% would be a reasonable upper limit for the initial fuel-melt fraction.
4. Last, the fraction of the debris' thermal energy that can be converted into mechanical work and therefore be able to damage CPBT is inherently limited by the second law of thermodynamics.

The net effect of the first three factors is assumed here to decrease the thermal energy available for CPBT damage by only a factor of 2 for the least severe type of meltdown and by 4 for the more

severe meltdowns. The factor governing the conversion of thermal to mechanical energy depends on the temperature of the debris and the temperature of the surroundings. If we assume that the water is in the same condition before and after the event (i.e., all the steam is condensed), we can express the available work in terms of properties of the debris:

$$W_a = (E_1 - E_0) - T_0 (S_1 - S_0) ,$$

where

W_a = available work,
 E_1 = final internal energy of the debris,
 E_0 = initial internal energy of the debris,
 S_1 = final entropy of the debris,
 S_0 = initial entropy of the debris,
 T_0 = initial temperature of the debris,
 T_a = the temperature of the surroundings = 373 K.

We can express the efficiency as

$$\text{eff} = 1 - T_a (S_1 - S_0)/(E_1 - E_0) ,$$

and we can simplify the entropy calculations by assuming a constant specific heat. For a single-phase solid or liquid metal,

$$d(\text{specific energy}) = C_p dT, \text{ and}$$

$$d(\text{specific entropy}) = C_p \ln (T_{\text{final}}/T_{\text{initial}}).$$

For the phase change (aluminum only),

$$d(\text{specific energy}) = \text{heat of fusion} = h_{fm}, \text{ and}$$

$$d(\text{specific entropy}) = h_{fm}/T_{\text{fusion}}.$$

The resulting expression for the theoretical thermal-to-mechanical energy conversion efficiency is

$$e = 1 - T_a \{ [F_x \ln(T_1/T_0) - h_{fm}/887] / [F_x (T_1 - T_0) - h_{fm}] \} ,$$

where

e = efficiency
 T_a = ambient temperature (373 K assumed),
 F_x = $(C_p, Al + C_p, \text{fuel} \times \text{fuel mass/aluminum mass})$.

We plug in the required specific heats and get the following maximum

theoretical efficiencies for three different scenarios:

Scenario	Initial temperature (K)	Final temperature (K)	Efficiency
Reactivity excursion without scram	1327	573	0.58
Inadequate cooling without scram	1684	573	0.64
Inadequate cooling on decay heat	873	573	0.53

Now we are ready to estimate the limiting amounts of energy that would be available to deform the CPBT in the event of a steam explosion for each scenario:

Scenario	Total thermal energy (MJ)	Available (MJ)
Reactivity excursion without scram	121	35.1
Inadequate cooling without scram	166	53.1
Inadequate cooling on decay heat	64.5	17.1

REFERENCE

1. F. Kreith, *Principles of Heat Transfer*, 2nd ed., International Textbook Company, Scranton, Pa., January 1966.

APPENDIX B

HYPOTHETICAL REACTIVITY EXCURSION WITHOUT SCRAM: LIMITING
DEBRIS TEMPERATURE AND ENERGY ESTIMATES

R. M. Harrington

B.1. INTRODUCTION**B.1.1 Containment Design Criteria**

The ANS containment systems shall be designed to withstand, without loss of containment capability, an ATWS. An anticipated transient is one that might be expected to happen over the 40-year life of the plant (probability $>0.5/40$ year, or equivalent probability $>0.0172/\text{year}$). The "without scram" means no control-rod insertion. With respect to fuel-coolant interaction (steam explosion, primarily), the reactivity-induced transient overpower event with failure of the scram system is the bounding case.

B.1.2 Implied Design Criteria

The implied design criteria with respect to reactivity insertion are as follows:

All-rod withdrawal (electronic failure): Reactivity insertion rate $< \$1.00/\text{s}$, and

Single-rod expulsion (mechanical failure): Reactivity insertion rate $< \$1.00/\text{s}$.

B.1.3 Reactivity Accident-Selection Criteria

Only physically possible reactivity accidents shall be chosen. The bounding fuel-coolant interaction is a $\$1.00/\text{s}$ ramp insertion of reactivity. Such an accident could come about as a result of multiple electronic failures that could cause all-rod withdrawal at the design withdrawal rate or mechanical failures that could expel a single rod at a greater-than-normal speed.

There are known mechanisms for the sudden step-like insertion of reactivity in quantities below the specified one-dollar design limit (e.g., primary beam-tube collapse).

B.1.4 Input Data Needed for Fuel-Coolant Interaction Calculations

The parameters that define the severity of a steam explosion are
(1) peak average fuel temperature during the reactivity excursion and
(2) the energy of the fuel melt that could be transferred violently to

the coolant. At present, no computer code can handle the whole accident; so the needed parameters are calculated using a combination of computer and hand calculations based on conservative assumptions, as outlined below.

B.2. CALCULATIONAL ASSUMPTIONS

1. The fuel temperature vs time following the reactivity insertion and up until the estimated point of burnout is calculated using the point kinetics model of J. March-Leuba. This model assumes minimal reactivity temperature feedback coefficients and no void feedback. Temperature vs time after burnout is hand calculated under the assumption of adiabatic heatup.
2. The thermal-hydraulic burnout point is assumed to occur when the average fuel temperature exceeds 500°C. There are several reasons why burnout should occur at or before this point, not the least of which is that the aluminum-based fuel becomes soft at >500°C.
3. The excursion is assumed to be terminated only when the fuel melt is swept from the core by the coolant flow. This assumption is conservative because there would be a significant negative reactivity compensation caused by the voiding that would accompany burnout. The relocation of fuel terminates the excursion for two reasons: (a) the individual fuel droplets are relocated into a lower flux region (the control rods are above the core) and (b) the negative reactivity is associated with the loss of fuel. The coolant flow rate is 13.5 m/s just upstream of the core inlet and 27 m/s between the plates. This is more than enough velocity to sweep out the molten fuel droplets and particles from the 1.27-mm-thick fuel plates. Because the normal flow direction is upward, there must be some slip between the molten debris and the flowing coolant to generate an upward force: a slip velocity of ~5 m/s would be enough to sweep 1.27-mm spherical melt droplets. The time required to sweep is based on a velocity of $13.5 - 5 \text{ m/s} = 8.5 \text{ m/s}$:

$$\text{Time} = \text{length/speed} = 0.5 \text{ m}/(8.5 \text{ m/s}) = 59 \text{ ms.}$$

The parameter length used above is the length of the core's active fuel region.

B.3. CALCULATIONS FOR THE \$1.00/s RAMP REACTIVITY INSERTION WITHOUT SCRAM

The computer-calculated transient results performed by J. March-Leuba are attached. (The results for one-dollar step insertion are not shown because they are less severe.) The hot spot fuel temperature reaches 500°C and possible burnout at ~0.6 s, at which time core prompt

power level equals 152%. The average fuel temperature reaches the 500°C burnout point at ~1.05 s, when core prompt power has reached 220%. The core is assumed to heat up adiabatically after 1.05 s and for (1) however long it takes to melt the fuel and (2) the 59 ms it takes for the debris to be swept from the core after it becomes molten. Hand calculations are used after the 1.05-s point. The hand-calculated temperatures and energies reported below use the specific heats and heats of fusion derived in Appendix A, which assumes a nominal 100% power of 350 MW in the 67.4-L active fuel volume.

Premelting

Energy required to reach the melting point, starting from normal average fuel temperature = $(600^{\circ}\text{C} - 300^{\circ}\text{C}) \times 0.1 \text{ MJ/K}$

$$= 30.1 \text{ MJ.}$$

Energy required to reach the melting point, starting from burnout = $(600^{\circ}\text{C} - 500^{\circ}\text{C}) \times 0.1 \text{ MJ/K} = 10 \text{ MJ.}$

Melting

Energy required to melt the fuel = 34.4 MJ.

Energy available from fuel-aluminum reaction = 8.2 MJ.

Net energy required for melting = 26.2 MJ.

Time required for the melting = $26.2 \text{ MJ} / (2.75 \times 350 \text{ MW})$,
 = 27.2 ms minimum,
 = $34.4 \text{ MJ} / (2.75 \times 300 \text{ MW})$, and
 = 35.7 ms maximum (without reaction).

(The power is taken at 275% - the estimated 220% plus a 25% uncertainty factor.)

Postmelting

Super-heating energy deposited during sweep-out = $59 \text{ ms} \times 2.20 \times 1.25 \times 350 \text{ MW} = 56.8 \text{ MJ.}$

Final average fuel temperature above molten = $56.8 \text{ MJ} / 0.125 \text{ MJ/K} = 454 \text{ K.}$

Final average fuel temperature = $600^{\circ}\text{C} + 454^{\circ}\text{C} = 1054^{\circ}\text{C.}$

Total core energy above normal = $30.1 \text{ MJ} + 26.2 \text{ MJ} + 56.8 \text{ MJ} = 113.1 \text{ MJ.}$

B.4 UNCERTAINTY ANALYSIS

The uncertainty in the peak fuel temperature and energy is believed to be +25% and -100%. The +25% allowance would be the possible result of more rapid reactivity insertion, higher burnout point, or longer sweep-out time of the fuel. The proceeding calculations of this appendix include this 1.25 conservatism; therefore, the accompanying energy release and peak fuel temperature estimates are considered to conservatively bound unmitigated reactivity excursions for ANS.

The -100% allowance represents the very real possibility that no steam explosion would occur at all. The initial boiling crisis and burnout would occur in the hotter portions of the fuel near the core exit (where the coolant more closely approaches saturation). As these hotter portions melt, they could be swept out over the ~400-ms period between initial hot spot melting and average fuel melting. Of course, less severe reactivity insertions could reduce the magnitude of the heatup and potential energy releases calculated previously.

The results reported here are intended to be representative of conservatively bound reactivity excursion ATWS events, but this cannot be verified until the reactivity excursion case is calculated with a computer code capable of (1) calculating the in-core voiding during the boiling that would precede burnout and (2) determining the effect of that voiding on the core-power level at the time of burnout.

APPENDIX C

WORKSHOP ON CAUSES AND PREVENTION OF MELT-WATER EXPLOSIONS

A workshop on steam-explosion phenomena was attended by the author of this report on July 29, 1988, at SNL. The purpose of this appendix is to provide an update on ongoing steam-explosion research efforts and to establish contact with other researchers.

C.1 WORKSHOP PARTICIPANTS

The workshop was attended by people from various industries, notably, aluminum, phosphorous, paper, and nuclear. An agenda of the meeting is provided as Exhibit C.1.

C.2 OVERALL CONCLUSIONS/MESSAGE OF WORKSHOP

1. Steam-explosion phenomena can be well characterized as evolving in four stages (i.e., mixing, triggering, propagating, and expanding). However, after 20 years of study, the mixing, triggering, and propagating stages are not well understood.
2. Analytical models developed to date are still crude because of the complexity of various stages that depict stochastic characteristics and are scale dependent. A state-of-the-art code IFCI is now under development at SNL and is expected to be released in ~1 year. However, "engineering" tools that have been used in the commercial reactor industry are available for design and safety studies.
3. The aluminum industry experiences several steam-explosion events each year, with several fatalities. Previous efforts over 20 to 30 years have involved brute-force experimentation under prototypical conditions to prevent explosions. Thinking now leans toward (1) evaluating various organic coatings for retardation of explosions and (2) allowing for several small steam explosions to avoid one "big" explosion.
4. Preliminary discussions were held with M. Berman (SNL) and M. Corradini (University of Wisconsin) to solicit their recommendations regarding ORNL's future efforts in studying the steam-explosion issue. Both indicated that ORNL needs to evaluate this issue carefully because of the very high power densities of ANS and the close parallels of these two designs with earlier plate-type aluminum-clad research reactors.

Communication was also established with M. L. Hyder of Savannah River Laboratory (SRL), who is also addressing the steam-explosion issue as part of a detailed severe-accident analysis program for their production reactors. Lee Hyder indicated a strong interest in discussing with ORNL topics of mutual interest and sharing information.

Exhibit C.1. Causes and Prevention of Melt-Water Explosions

Sandia National Laboratories
 Albuquerque, New Mexico
 Friday, July 29, 1988

FINAL PROGRAM

<u>Topic</u>	<u>Presenter</u>
Introduction	M. Berman, Sandia National Laboratories
Industrial Incidents and Concerns	(Chair - M. Berman)
Aluminum	S. C. Epstein, Aluminum Association
Phosphorus	L. E. Loviza, Monsanto Soda Springs, Idaho
Smelt	J. V. Gommi, Weyerhaeuser Tacoma, Wash.
Steam Explosions in Industrial Granulation Processes for Ferroalloys (FeSi, FeMn, etc.)	J. G. Thuestad, Elkem Norway
Production Reactors	M. L. Hyder, Savannah River Laboratory Aiken, S.C.
Research Programs	(Chair - R. P. Anderson)
U.S. Aluminum Industry	R. E. Miller, ALCOA Pittsburgh, Pa.
Metal-Water Interactions and Vapor Explosions	M. L. Corradini, University of Wisconsin Madison, Wis.
Thermite-Water Interactions	D. F. Beck, Sandia National Laboratories
Laboratory Studies of Aluminum-Water Interactions	L. S. Nelson, Sandia National Laboratories

Exhibit C.1 (continued)

FINAL PROGRAM

<u>Topic</u>	<u>Presenter</u>
Mechanisms	(Chair - M. L. Corradini)
Mechanisms of Steam Explosions	J. H. Lee McGill University Montreal, Canada
An Evolving Picture of Vapor Explosion Mechanisms	R. P. Anderson Argonne, Ill.
Surface Triggering	E. W. Dewing, Alcan Kingston, Ontario
Thermodynamic and Fluid-Dynamic Modeling of 2ϕ Propagating Explosions	M. Berman, Sandia National Laboratories
Discussion	
Adjourn	
Tour of FITS and VAT Sites	

Internal Distribution

- | | |
|---------------------|--------------------------------------|
| 1. S. H. Buechler | 17. F. J. Peretz |
| 2. D. J. Cook | 18. D. L. Selby |
| 3. W. G. Craddick | 19. D. B. Simpson |
| 4. G. F. Flanagan | 20. A. Sozer |
| 5. E. C. Fox | 21. R. P. Taleyarkhan |
| 6. S. R. Greene | 22. P. B. Thompson |
| 7. R. C. Gwaltney | 23. B. D. Warnick |
| 8. R. M. Harrington | 24. C. D. West |
| 9. S. A. Hodge | 25. G. T. Yahr |
| 10. F. J. Homan | 26. A. Zucker |
| 11. C. R. Hyman | 27. ORNL Patent Section |
| 12. J. E. Jones Jr. | 28. Central Research Library |
| 13. B. S. Maxon | 29. Document Reference Section |
| 14. D. L. Moses | 30-31. Laboratory Records Department |
| 15. D. G. Morris | 32. Laboratory Records, RC |
| 16. B. W. Patton | |

External Distribution

33. G. Allison, Idaho National Engineering Laboratory, P.O. Box 1625, Idaho Falls, ID 83415
34. L. Y. Cheng, Brookhaven National Laboratory, Bldg. 703, Department of Nuclear Energy, Upton, NY 11973
35. D. Croucher, Idaho National Engineering Laboratory, P.O. Box 1625, Idaho Falls, ID 83415
36. M. L. Hyder, Reactor Safety Research Division, Westinghouse Savannah River Company, Savannah River Laboratory, Aiken, SC 29808
37. J. E. Kelley, Sandia National Laboratory, Division 6418, P.O. Box 5800, Albuquerque, NM 87185
38. R. T. Lahey, Jr., Department of Nuclear Engineering and Engineering Physics, Jonsson Engineering Center, Rensselaer Polytechnic Institute, Troy, NY 12180-3590
39. I. Madni, Brookhaven National Laboratory, Bldg. 703, Department of Nuclear Energy, Upton, NY 11973
40. M. Z. Podowski, Department of Nuclear Engineering and Engineering Physics, Jonsson Engineering Center, Rensselaer Polytechnic Institute, Troy, NY 12180-3590
41. D. A. Sharp, Reactor Safety Research Division, Westinghouse Savannah River Company, Savannah River Laboratory, Aiken, SC 29808
42. P. R. Tichler, Brookhaven National Laboratory, Bldg. 703, Department of Nuclear Energy, Upton, NY 11973

43. A. L. Wooten, Reactor Safety Research Division, Westinghouse Savannah River Company, Savannah River Laboratory, Aiken, SC 29808
44. Office of Assistant Manager for Energy Research and Development, Department of Energy, ORO, P.O. Box 2001, Oak Ridge, TN 37831
- 45-54. Office of Scientific and Technical Information, P.O. Box 62, Oak Ridge, TN 37831